Initial study of seismic ground vibration data from mega-watt class wind turbines

Interim Technical Report

June 2013

The views expressed in this interim report are preliminary and subject to review and validation. This report is therefore prepared on a without prejudice basis, for the sole purpose of assisting the Eskdalemuir Working Group. Full quantitative analysis is envisaged as part of the substantive research outlined in the Technical Proposal agreed by the Eskdalemuir Working Group in November 2012.

Summary

To safeguard the seismometer array at Eskdalemuir (EKA) from interference from seismic ground vibration (SGV) from wind turbines, a consultation zone for wind farm development is defined between 10 and 50km from the cross-over point of the two arms of EKA. The safeguards were recommended by the original Eskdalemuir Working Group (EWG) in 2005, relying on commissioned research (Styles *et al.* 2005). The 2005 model utilised measurement of the vertical component of SGV in 2004 from 26 stall-regulated wind turbines, at Dun Law wind farm, each turbine with rated-power of 0.66 megawatt (MW), and is based on a narrow-frequency approximation at 4.5Hz.

On 27 February 2012 a reconvened EWG, chaired by the Scottish Government, considered a staged approach to the technical work required to re-examine the 2005 model. Following a request from industry the EWG agreed a “Stage Zero” of the technical work “for an initial piece of work which would inform the fuller research stages referred to at the meeting”. This is the interim report for the “Stage Zero”, or initial study described in the technical proposal agreed by the reconvened EWG at its meeting on 2 November 2012 (EWG 2012b).

A review is presented of previous studies of SGV from stall- and pitch-regulated wind turbines. The experiment to acquire far-field SGV from Craig wind farm in 2011 is described. Craig wind farm comprises four pitch-regulated turbines, each with a rated-power of 2.5MW — these data are considered pertinent to re-examining the 2005 model, as it is pitch-regulated turbines that have been constructed in the consultation zone.

Preliminary analysis of the Craig 2011 SGV data show far-field vertical-component SGV power spectra with clear peaks at integer multiples of the blade-passing frequency (around 0.85Hz) — this observation is diagnostic of SGV from operating wind turbines. The peak with the highest power is at a frequency around 1.7Hz, corresponding to the second multiple of the blade-pass frequency. The power in the spectral peaks at higher frequencies decreases with increasing blade-pass frequency multiple. The frequency and power of each spectral peak, associated with multiples of the blade-pass frequency, increases with increasing wind speed. This strongly suggests that the dominant far-field SGV from pitch-regulated turbines is generated by the action of the turbine blades passing the tower, and not by excitation of structural vibration modes.

MW-class pitch-regulated turbine blades rotate at a slower rate than stall-regulated turbines, and thus have a lower blade-pass frequency (around 0.85Hz and 1.4Hz respectively). The passband for the detection of signals of interest by EKA is around 0.5-8Hz. Therefore the SGV from pitch-regulated turbines will have a larger number of more closely spaced spectral peaks at multiples of the blade-pass frequency in the passband of interest, than the SGV from stall-regulated turbines. Thus, the narrow-frequency approximation, as in the 2005 model, should be re-examined and frequency-distance weighting of the SGV spectra is required.

Frequency-distance weighting theory has been developed based on optimal signal detection theory, and the physical properties of signals of interest and noise at EKA derived from observations. The propagation term in the frequency-distance weighting model uses the parameters adopted in the model of Styles *et al.* (2005). The resulting weighting function requires a calibration or normalisation factor that depends on its application.

For the purposes of this interim report the frequency-distance weighting developed is calibrated or normalised with respect to the 1.5-4.5Hz bandpass filter used to determine the threshold of 0.336 nanometres. The threshold is used in the current MOD safeguarding approach. It should be noted that the “finalised” weighting function, ultimately used in the substantive Stage One research to quantify any “headroom” to accommodate further wind farm development in the consultation zone, could be for a different application to that considered here (for example, a revised definition of the threshold), and thus may

require a different calibration.

The SGV predicted by the 2005 model, at a range of distances within the consultation zone, is compared with preliminary estimates from the frequency-distance weighted SGV spectra calculated from data recorded at the two quietest sites during the Craig 2011 field experiment for wind speeds in the range 11-12m/s. The ratio of the 2005 model prediction to the preliminary estimated SGV can be thought of as the apparent overestimate of the source-term in the 2005 model. The size of the apparent overestimate depends on distance. Preliminary estimates of ratios, subject to independent validation and further research, are around eight at a distance of 10km, reducing to ratios around unity (i.e., no difference) at a distance of 50km. However, further consideration of possible bias due to direction and/or site effects, and other factors, such as the mode of SGV propagation, is required.

Subject to independent validation by the FMB/EWG commissioned consultant (EWG 2012b) and further work during this initial study, these interim preliminary results support the view that it is likely to be worthwhile pursuing the substantive research into re-examination of the 2005 model, as envisaged in Stage One of the technical proposal (EWG 2012a). The substantive research stage would quantify any “headroom” to accommodate further wind farm development in the consultation zone, and develop a mathematical model to be implemented in a software tool to enable effective safeguarding of EKA.

Contents

1 Introduction

The seismometer array at Eskdalemuir (EKA) in the southern uplands of Scotland is part of the UK's contribution to the 321 stations in the International Monitoring System (IMS) network. The IMS is part of the Comprehensive Nuclear-test-Ban Treaty (CTBT) verification regime, and the UK is required by the treaty to safeguard its IMS stations.

To safeguard EKA from interference from seismic ground vibration (SGV) from wind turbines, a consultation zone for wind farm development is defined between 10 and 50km from the cross-over point of the two arms of EKA. The safeguards were recommended by the original Eskdalemuir Working Group (EWG) in 2005, relying on commissioned research (Styles *et al.* 2005), utilising measurement of the vertical component of SGV in 2004 at Dun Law wind farm, which at that time comprised 26 stall-regulated turbines with rated-power of 0.66 megawatt (MW).

The 2005 model (Styles *et al.* 2005) is used to predict the SGV from wind turbines in the zone. The 2005 model is a narrow-frequency approximation around 4.5Hz, with a source term that depends on the turbine rated-power, and a propagation term that depends on the distance of the turbine from the EKA cross-over. Under the safeguards the cumulative SGV of permitted wind turbines in the zone is not allowed to exceed a threshold of root-mean square (rms) displacement of 0.336 nanometres (nm) — the value taken as the SGV at EKA at windy times (Styles *et al.* 2005).

The MoD's wind farm safeguarding approach is to not object to wind farm development on a first-come, first-served basis until the threshold is reached. This approach provisionally allocates a proportion of the SGV threshold to a wind farm development, calculated using the 2005 model, considering the contribution from each individual turbine in the development. A development is not objected to if the cumulative SGV is less than the threshold.

Since 2005, wind farm developments in the consultation zone with a total of over 950MW of electrical generating capacity have not been objected to by MOD. The wind farms so far constructed in the zone are of large MW-class pitch-regulated turbines.

Recent modelling studies predict that different modes of turbine vibration give rise to far-field SGV levels that vary with direction, indicating that SGV from wind turbines measured by seismometers in a line in a single direction, such in the 2004 Dun Law experiment, may be biased. In mid-2011 an experiment was conducted at Craig wind farm, about 20km from EKA, with eight seismometers approximately equally distributed in di-

rection around four 2.5MW pitch-regulated wind turbines. Analysis of these new data, along with those acquired in 2004, can re-examine the 2005 model recommended by the EWG.

Preliminary analysis of the 2011 data indicates that the turbines at Craig generated far-field vertical-component SGV with multiple spectral peaks at frequencies lower than 4Hz, each peak with larger power than the spectral peaks in the 4-5Hz band. The total SGV propagated by wind turbines could then be reassessed against that predicted by the 2005 model. Re-examination of the Styles model would ensure that it is appropriate for MW-class pitch-regulated wind turbines constructed in the consultation zone.

On 27 February 2012 a reconvened EWG, chaired by the Scottish Government, considered a staged approach to the technical work required to re-examine the 2005 model. The EWG agreed a "Stage Zero" of the technical work "for an initial piece of work which would inform the fuller research stages referred to at the meeting".

A technical proposal (EWG 2012a) for the initial study was agreed by the EWG at its meeting on 2 November 2012. The aim of the "Stage Zero" technical work is to analyse the far-field seismic data from the mid-2011 Craig wind farm experiment, and test and develop the methodology described below. At its meeting on 2 November 2012 the EWG proposed that the part of the initial study, conducted using MOD resources, would be consolidated with initial technical work by contractor(s) into a "Stage Zero final report". This is the interim report describing the initial study work performed by AWE (on behalf of MOD).

2 Previous studies of seismic ground vibration from wind turbines

2.1 Stall-regulated turbines

The first main result of the Styles *et al.* (2005) study identified that the SGV observed from the stall-regulated ("fixed-speed") turbines at Dun Law wind farm was attributed to propagation of seismic Rayleigh waves, rather than infrasound (sound waves with frequencies $<$20Hz) propagating in the air and coupling to the ground as proposed by Schofield (2001). Styles *et al.* (2005) identified multiple spectral peaks in the Dun Law far-field vertical-component SGV data, corresponding to harmonics (or integer multiples) of the turbine blade-pass frequency; about 1.4Hz for a typical rotation rate of 28

revolutions-per-minute (rpm).

When the turbines were operating, harmonic peaks in the power spectrum of SGV data recorded by a seismometer at the Kelphope 1 site, are observed at frequencies of approximately 2.8, 4.3, 5.7, 7.1 and 8.5Hz. The Vesta V47 turbines at Dun Law have a 10% variability in rotation rate which will result in corresponding variability in the frequencies of the harmonics observed. Notably the harmonic spectral peaks observed at Dun Law were not present when the turbines were not operational, indicating that, along with harmonic seismic observations at other wind farms previously made by Professor Styles and reported in Styles *et al.* (2005), that the observation of harmonic spectral peaks is diagnostic of SGV from wind turbine operation.

The second main result of the Styles *et al.* (2005) study was the development of the 2005 model summarised above, that is used to safeguard EKA. Details of how the 2005 model source-term is determined are pertinent to the initial study and substantive Stage One research described in EWG (2012a), and are described below.

The narrow-frequency approximation of 4.5Hz was selected for the 2005 model, because, (1) the 4-5Hz band is quiet at EKA, and (2) the 4-5Hz frequency band is also where SGV was thought to be efficiently generated by wind turbines, based on experience with the Dun Law data, the study of Schofield (2001), and previous studies reported by Styles *et al.* (2005).

The wind turbines at Dun Law and at the Stateline wind farm, studied by Schofield (2001), are stall-regulated Vesta V47 0.66MW turbines. The source-term is determined from SGV root-mean square (rms) levels derived from the area under the spectral peak around 4.3Hz from observations, at the Kelphope 1 and Kelphope 2 sites at Dun Law (page 86 of Styles *et al.* 2005), and the spectra corresponding to SGV observations at Sites 7 and 10, at distances of 720m and 18,270m from turbine HGA-1 at Stateline wind farm respectively (Figure 7 of Schofield 2001, and Table 7 on page 88 of Styles *et al.* 2005).

The areas under the 4.3Hz spectral peaks from the Dun Law observations were determined interactively using a computer graphical user interface (see page 125 of Appendix D in Styles *et al.* 2005) from the Power Spectral Density (PSD) of the vertical component of the SGV, and the square-root taken. By Parseval's theorem this is equivalent to the rms SGV for the narrow pass band corresponding to the width of the spectral peak. The units of nm for the rms SGV indicate that the PSD were in units of nm^2/Hz, and were for vertical-displacement ground motion.

The area under the 4.3Hz spectral peaks from Sites 7 and 10 at Stateline was measured from Figure 7 of Schofield (2001), by approximating the peak as a triangle and squaring the values of the three points and calculating the area, since the labelled units on the ordinate are in m/$\sqrt{\text{Hz}}$. The square-root of the area of this approximate PSD peak is in units of m. This is then the rms SGV for displacement ground motion, but for the horizontal motion in the direction of the nearest turbine (the horizontal-radial direction).

Rayleigh waves propagate with a retrograde elliptical particle motion, with seismic energy on the vertical and horizontal-radial components (the radial direction is along the great-circle path from the source to the receiver). The consistency of narrow-frequency source-terms determined from the vertical SGV data at Dun Law and the horizontal-radial SGV data from Stateline, reported by Styles *et al.* (2005), suggests Rayleigh wave propagation, and that local geological conditions in the vicinity of the respective wind farms play only a second-order effect on the measured SGV. Further, while uncertainty is not formally treated by Styles *et al.* (2005), the consistency of the source-terms derived from the two independent data sets was taken as an indicator, by the original EWG, that the source term in the 2005 model was reasonable, while acknowledging the caveat of Styles *et al.* (2005) that the source-term and model are based on measurements from stall-regulated turbines available at the time of the field work in 2004.

During testing of the measurement method[1] described below, in late-2011, data from the Dun Law experiment were analysed from 5-7 October 2004. This analysis indicates that the PSD shown in Styles *et al.* (2005) are for ground *velocity* not displacement — this has implications for the source term in the 2005 model.

Figure 1 shows the vertical-component PSD calculated for the time period 0000 to 0100 GMT on 19 September 2004 recorded at the Kelphope 1 site, about 2.3km from the nearest turbine in the Dun Law wind farm. With the ordinate in dB (decibels), these are the same data used to produce Figure 30 on page 40 of Styles *et al.* (2005). The average wind speed at Dun Law wind farm for this time period was 11.1m/s. The PSD in Figure 1 clearly show the presence of the harmonics, at frequencies around 2.8, 4.3, 5.7, 7.1, and 8.5Hz, that are integer multiples of the turbine blade-pass frequency (around 1.4 Hz), and are diagnostic of SGV from operating wind turbines. The green line shows the PSD in dB relative to the velocity power of seismic ground vibration in units of $(\text{m/s})^2/\text{Hz}$. The red line shows the PSD in dB relative to displacement power in units of m^2/Hz. A comparison of the green line in the Figure with the green line in Figure 30 on page 40

[1] Originally conducted in support of development of a measure of the effectiveness of the Seismically Quiet Tower mitigation technology.

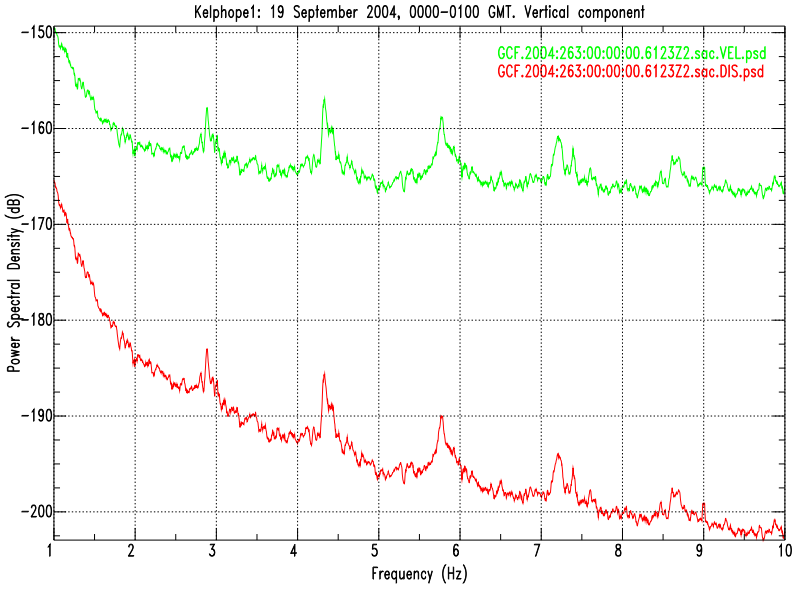

Figure 1: Power Spectral Density (PSD) in decibels (dB) from the Kelphope 1 site about 2.3km from Dun Law wind farm. Seismic ground vibration PSD in dB relative to velocity power in units of $(m/s)^2/Hz$ (green spectrum), and dB relative to displacement power in units of m^2/Hz (red spectrum) are shown.

of Styles *et al.* (2005) demonstrates that the dB in Figure 30 in Styles *et al.* (2005) are relative to velocity in units of $(m/s)^2/Hz$. This also raises the question as to whether Schofield (2001) used velocity or displacement.

The technical proposal (EWG 2012a) has attempting to resolve these issues as a task for the substantive Stage One research, by comparing the results of the analysis of the 2011 Craig data, with the results from the 2004 Dun Law and Stateline experiments.

2.2 Pitch-regulated turbines

Recently Fiori *et al.* (2009) and Saccorotti *et al.* (2011) report seismic measurements taken at the turbine base and in the far-field from MW-class pitch-regulated turbines in Germany and Italy respectively. The pitch-regulated turbines studied by Fiori *et al.* (2009) rotate between 9.5 to 20 rpm, corresponding to blade-pass frequencies between 0.48Hz and 1Hz. Thus, the expectation is for more harmonic peaks, in the broadband of frequencies of interest (0.5-8Hz) for nuclear test monitoring using EKA (EWG 2012a), from the slower rotating pitch-regulated turbines than from faster rotating stall-regulated turbines.

Both the German site 25km from Hamburg, and the Italian site 15km from Pisa, have relatively high ambient seismic noise levels at night time, with PSD levels at 2Hz about 10dB below the model used to characterise the seismically noisiest sites (the New-High-Noise Model of Peterson 1993). Both sites have high anthropogenic noise levels during day time. At night time these sites are some 30dB noisier around 2Hz compared with EKA, which has average levels at 2Hz for wind speeds around 12m/s (at a height of 50m) that are about 20dB above the model that characterises the seismically quietest sites (the New-Low-Noise Model of Peterson 1993). (A 30dB difference equates to a factor of 1000 in power.) Nonetheless, Saccorotti *et al.* (2011) report an analysis of the PSD of the data, recorded at a reference site near the wind farm studied, that shows that the greatest power is in a peak around 1.7Hz (see Figure 6 of Saccorotti *et al.* 2011). However, the diagnostic harmonic spectral peaks in the far-field SGV are not clear, presumably obscured by the high ambient seismic noise levels.

3 Seismic ground vibration data from the 2011 experiment

3.1 Background

The Craig seismic data set was acquired in mid-2011, to support research into mitigation technology being proposed by Wind Energy (Newfield) Ltd. The field work was conducted by staff from the Applied and Environmental Geophysics group at the University of Keele (headed by Professor Styles), SeisUK (who provided five seismometers) at the University of Leicester, XiEngineering, EKA and AWE (who provided three seismometers). The cooperation of Craig Wind Farm Ltd, and Mr Pringle, land manager, for permission to deploy seismometer 6028 (site AEG-1 in Table 1) in the forest to the west, is acknowledged.

A network of eight seismometers was deployed around the four turbines at Craig Wind Farm, referred to as “T1”, “T2”, “T3”, and “T4”, using the method described by Brisbourne *et al.* (2011). T1 has the prototype Seismically Quiet Tower (SQT) mitigation technology installed. The Craig experiment included partial and complete shutdown experiments, including times with only an individual turbine running, from 20-22 May and 15-18 July 2011.

Site	Date deployed	OS East	OS North	Inst. type	Inst. ref	Distance in m from T1	T2	T3	T4
AEG-0	16-05-11	32376	87047	6TD	6028	1249	1075	1077	953
AEG-1	18-05-11	31395	86044	6TD	6028†	1084	871	588	515
AEG-2a	16-05-11	32575	86521	6TD	6188‡	732	626	760	758
AEG-2b	25-05-11	32662	86419	6TD	6099	654	595	776	810
AEG-3	17-05-11	33117	85535	6TD	6159	717	962	1243	1430
AEG-4	17-05-11	32946	85308	6TD	6140	698	957	1212	1421
AEG-5	26-05-11	32302	87061	6TD	6351	1270	1084	1066	929
GSL-1	16-05-11	31704	86495	40TD	4t50	1020	761	530	307
GSL-2	16-05-11	31994	87247	40TD	4421	1517	1297	1203	1016
GSL-3	17-05-11	33143	86491	3ESP	3y96	978	1019	1243	1296

Table 1: Seismometer deployment for the Craig experiment. † seismometer at site AEG-0, reference, 6028 re-deployed to site AEG-1, due to animal interference. ‡ Site AEG-2a moved about 100m to AEG-2b due to animal interference, instrument replaced on 25-05-2011 by a 6TD with instrument reference 6099.

3.2 Seismometer deployment

Table 1 gives the UK Ordnance Survey (OS) grid references, deployment dates, and distances to each of the four turbines at Craig wind farm. Figure 2 shows the location of the turbines and seismometers. These are Nordex N80 2.5MW rated power pitch-regulated turbines. The table also the instrument type and reference number.

Examination of the instrument responses shows that all the seismometers deployed (listed in Table 1) have a response that is proportional to ground velocity motion over the frequency passband considered in this study. Table 2 gives the calibration value “CALIB” which is the conversion factor from digital counts (the output of the digitiser) to ground velocity in nm/s. Thus, to obtain ground velocity the digital seismic data are multiplied by the relevant CALIB value.

4 Calculation of power spectra

4.1 Preliminary analysis

Figure 3 shows the resulting power spectrum from a preliminary analysis of the Craig vertical SGV data recorded at Site GSL-1. The displacement power spectrum was calculated from a 30 minute segment where the wind speed was around 12m/s, and all

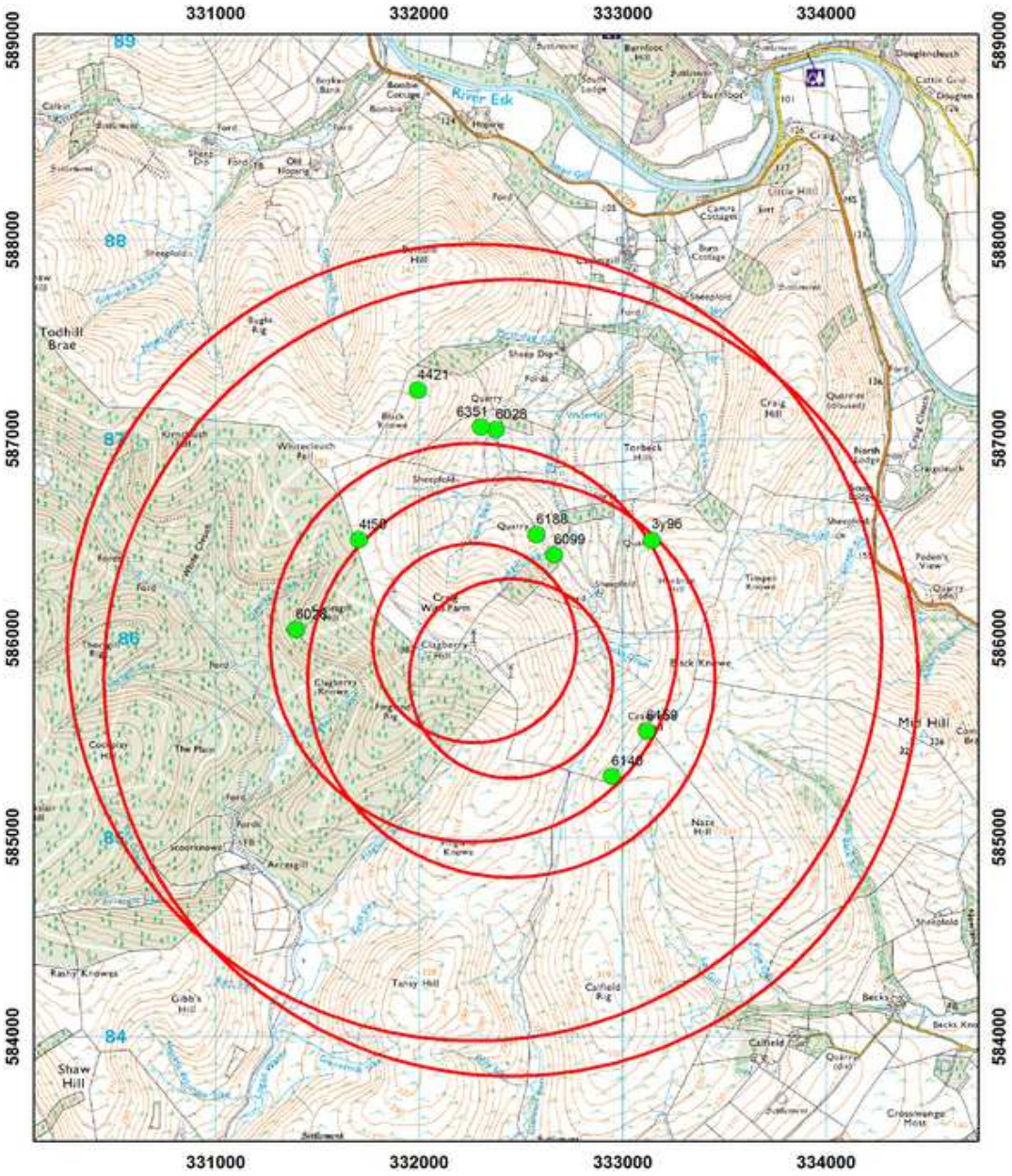

Figure 2: Location of the seismometers, referenced by instrument reference number in Table 1, overlain on the OS 1:25000 base map. The red circles are at distances of 500m, 1000m and 2000m from T1 (the turbine furthest south) and T2. The turbine furthest north is T4. T3 is not marked on this OS map. (Courtesy of Professor Styles, University of Keele.)

Site	Date deployed	OS East	OS North	Inst. type	Inst. ref		Digitiser. ref	CALIB (nm/s/count)
AEG-0	16-05-11	32376	87047	6TD	6028	Z	–	–
AEG-1	18-05-11	31395	86044	6TD	6028	Z	C1132	0.4027
AEG-2a	16-05-11	32575	86521	6TD	6188	Z	C949	0.4067
AEG-2b	25-05-11	32662	86419	6TD	6099	Z	A828	0.4125
AEG-3	17-05-11	33117	85535	6TD	6159	Z	C939	0.4033
AEG-4	17-05-11	32946	85308	6TD	6140	Z	C1134	0.4030
AEG-5	26-05-11	32302	87061	6TD	6351	Z	B417	0.4053
GSL-1	16-05-11	31704	86495	40TD	4T50	Z	A2888	1.019
GSL-2	16-05-11	31994	87247	40TD	4421	Z	A1453	1.014
GSL-3	17-05-11	33143	86491	3ESP	3Y96	Z	A2895	0.5542

Table 2: Calibration factors “CALIB” for the seismometers deployed in the Craig experiment.

four turbines at Craig wind farm were generating electrical power. There are clear harmonic spectral peaks, with a fundamental around 0.85Hz (equivalent to a rate of around 17 rpm), characteristic of far-field SGV attributed to wind turbine operation. It is also clear that the vast majority of SGV power attributed to wind turbine operation of these pitch-regulated Nordex N-80 turbines (2.5MW rated power) is concentrated at frequencies lower than 4.5Hz (the frequency at which the 2005 model is based), with apparently increasing SGV power in the lower harmonics.

The preliminary power spectrum in Figure 3 indicates that the 2005 model may need re-examining for MW-class wind turbines in the consultation zone. However, multiple power spectra, normalised as Power Spectral Density (PSD), need to be calculated, and averaged in a statistically robust way, to firstly determine if this preliminary PSD is anomalous, and secondly if initial quantitative analysis can determine if there are prospects for “headroom” to accommodate further large wind turbine development in the consultation zone.

4.2 PSD calculation

Styles *et al.* (2005) demonstrated that the far-field SGV from a wind turbine can be considered as a pseudo-stationary harmonic signal, i.e., we assume that the SGV from a wind turbine is stationary, at least over the 10 minute time window associated with the wind speed/direction and power generation data.

The method is based on estimation of the normalised displacement PSD from a 10

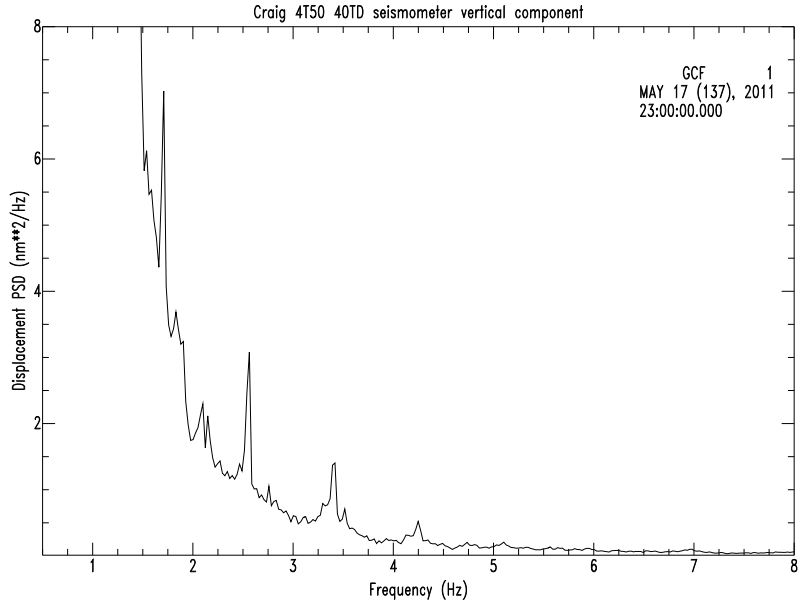

Figure 3: Example of preliminary displacement PSD from the vertical component of the 40TD seismometer 4T50 for a 30 minute time segment starting at 2300 UTC on 17 May 2012. Note the harmonic spectral peaks around 1.7, 2.55, 3.4, and 4.25Hz. The wind speed at hub height was around 12m/s.

minute SGV time series recorded by a seismometer, associated with a wind speed and an operating mode at Craig wind farm (for example, all four turbines generating electricity). The normalisation of the power spectrum is such that the PSD units are in nm^2/Hz. The displacement PSD associated with a range of wind speed (for example in bins 1m/s wide) and operating mode, are averaged using robust statistics to obtain a smoothed displacement PSD for a particular site, wind speed range and operational mode.

The following steps are followed in the PSD calculation,

1. The digital vertical-component SGV data from each seismometer has the mean value removed, and is then converted to velocity in the time domain (by multiplying by the CALIB values in Table 2). The time series are discretised into 10 minute time segments corresponding to the 10 minute average wind speed values from the turbine hub. For operational modes where more than one turbine is generating electrical power the maximum wind speed is chosen.

2. The digital data are down-sampled to 50 samples/s using a digital anti-alias filter (from the original sampling rates of 200 and 100 samples/s for the 6TD and other seismometer instrument types respectively).

3. The PSD for the 10 minute data segment from each seismometer is calculated using Welch's method with a data window overlap of 50%. A half-window length of 20.48s (1024 samples at 50 samples/s), gives K=28 overlapping data windows. This approach is near-optimal, and reduces the variance of the resulting Welch PSD relative to that of a naive single 20.48s PSD by about 9K/11, or a factor of about 23 (Press *et al.* 1992).

4. The resulting velocity PSD is transformed to a displacement PSD by integration in the frequency domain (dividing by $(2\pi f)^2$), and normalised (multiply by 2048/50) to give units of nm^2/Hz.

4.3 Robust PSD estimation

The expectation is that the phase of the SGV from each wind turbine in a farm is random (Styles *et al.* 2005), so averaging of individual displacement PSD from 10 minute segments is required to estimate the underlying power spectrum. Here we consider only times when all four of the turbines at Craig are generating electricity — this results in the number of 10-minute PSDs for each station and 1m/s wind-speed as indicated in Table 3.

For each site and wind-speed bin we calculate the inter-quartile mean (a type of "robust statistics") at each discrete frequency, resulting in a smoothed displacement PSD. Additional calculation of the mean, median, and 25th and 75th percentiles gives an indication of the underlying distribution.

Figure 4 shows two examples comparing the arithmetic mean, with the median and inter-quartile mean for the wind speed range 11-12m/s at sites GSL-1 and AEG-5. It is clear that the median and inter-quartile mean estimates of the underlying average PSD at site GSL-1 (Figure 4a) agree closely. The arithmetic mean is biased high towards the 75th percentile, and the 75th and 25th percentiles bound the median values within an acceptable range, indicating a well behaved inter-quartile sample distribution. We also note that the estimates of the median PSD closely match the PSD in Figure 3 confirming that the preliminary power spectrum, with harmonic peaks around 1.7, 2.55, 3.4, and 4.25Hz, is characteristic of the SGV PSD from wind turbines for wind speeds around 12m/s.

The median and inter-quartile mean estimates of the PSD for site AEG-5 (Figure 4b) agree closely. The arithmetic mean is biased high, especially for frequencies above

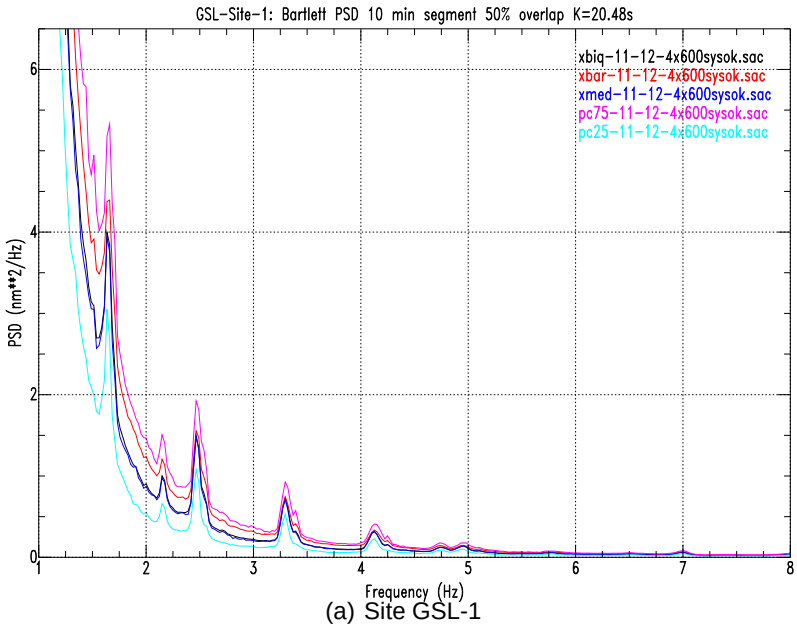

(a) Site GSL-1

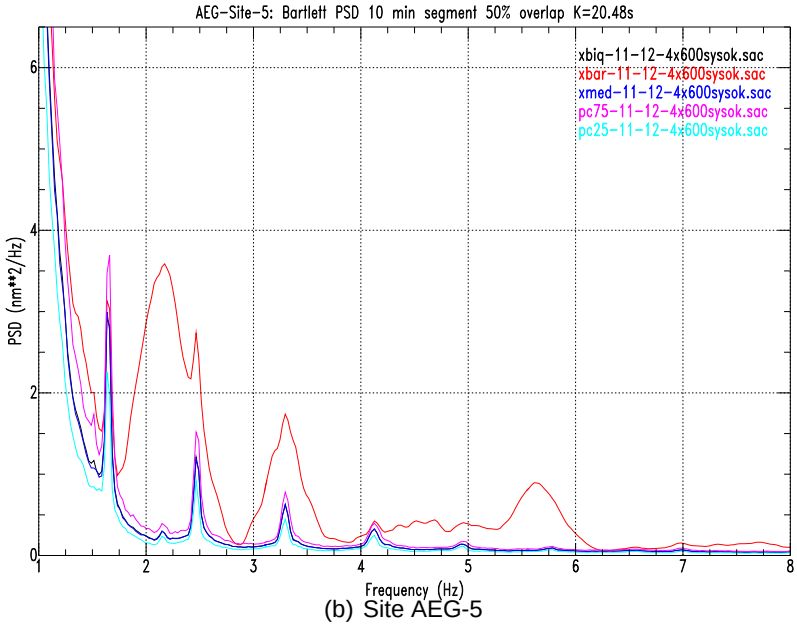

(b) Site AEG-5

Figure 4: Examples of averaged displacement PSD from (a) Site GSL-1 and (b) AEG-5 for the wind speed bin 11-12m/s. “xbiq” is the inter-quartile mean, “xmed” is the median, “xbar” is the arithmetic mean, “pc75” and “pc25” are the 75th and 25th percentiles respectively.

Wind speed	Site reference							
(m/s)	AEG-1	AEG-2b	AEG-3	AEG-4	AEG-5	GSL-1	GSL-2	GSL-3
5-6	252	277	209	244	497	497	490	450
6-7	218	246	206	214	449	488	475	443
7-8	183	193	187	182	320	399	395	328
8-9	163	153	170	160	210	327	319	230
9-10	133	95	145	135	126	243	237	162
10-11	174	117	182	178	137	292	286	197
11-12	169	108	181	177	145	295	294	222
12-13	128	57	146	142	81	213	213	160
13-14	118	56	136	131	43	161	161	111
14-15	51	22	59	58	14	68	68	44
Total	1589	1324	1621	1621	2022	2983	2938	2347

Table 3: Number of 10-minute PSDs calculated at each site when all four turbines at Craig are generating electricity cut by wind speed bin.

1.5Hz. However, the 75th and 25th percentiles bound the median values within an acceptable range, indicating a well behaved inter-quartile sample distribution. The biased arithmetic mean indicates that overall the sample distribution has a long high-end tail, but it seems clear that the inter-quartile mean is an effective robust estimate. In the following analysis we adopt the inter-quartile mean as the best estimate of the underlying power spectrum.

Figure 5 shows plots of the inter-quartile mean vertical displacement PSD from the two quietest sites showing clear harmonic peaks at integer multiples of the blade-pass frequency (around 1.7, 2.55, 3.4, and 4.25Hz) characteristic of the SGV from wind turbines. The power in the spectral peaks increases with increasing wind speed measured at the turbine hub height. The harmonic peak frequency also increases with increasing wind speed, consistent with the blade rotation rate of the pitch-regulated turbines increasing with increasing wind speed.

One exception is a small peak around 2.15Hz that is not associated with an integer multiple of the blade-pass frequency. While the power in this peak increases with increasing wind speed, the peak frequency does not increase with increasing wind speed.

Figure 6 shows logarithmic plots of the inter-quartile mean vertical displacement PSD from two of the sites that seem to be susceptible to wind-generated ambient background noise. The harmonic peaks characteristic of the SGV from wind turbines are seen at intermediate wind speeds, but tend to be dominated by what appears to be broadband ambient background noise at higher wind speeds (above 12m/s).

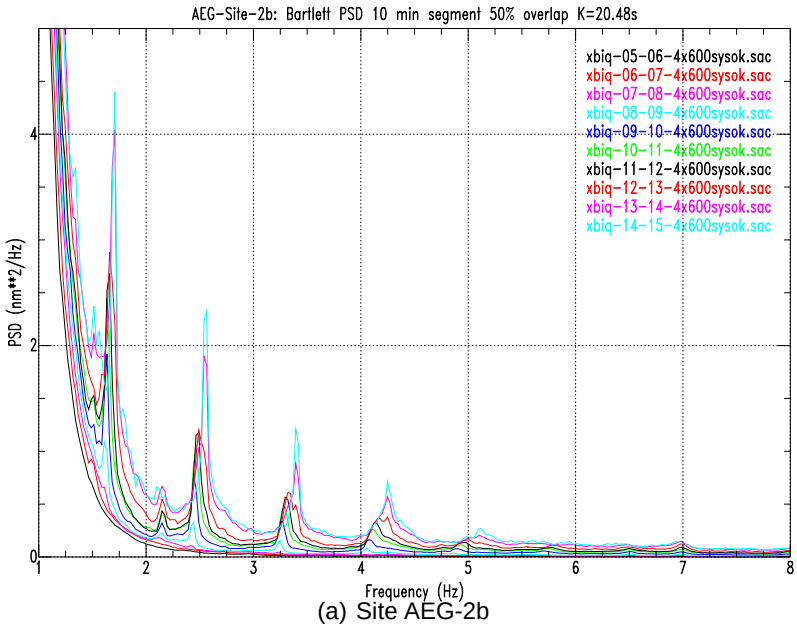

(a) Site AEG-2b

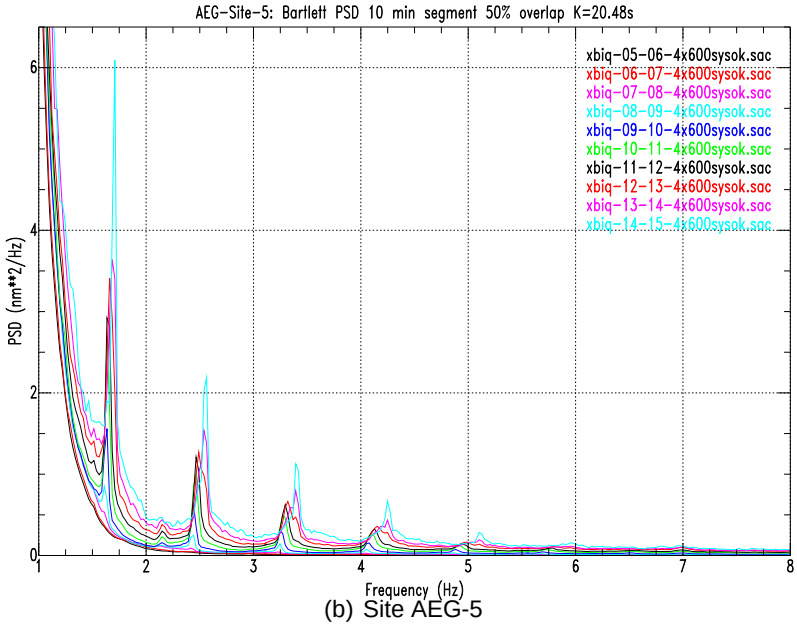

(b) Site AEG-5

Figure 5: Inter-quartile mean vertical displacement PSD from the two quietest sites showing clear harmonic peaks characteristic of the SGV from wind turbines, (a) AEG-2b, and (b) AEG-5, for a range of wind speeds in bins of 1m/s when all four turbines at Craig are generating electricity.

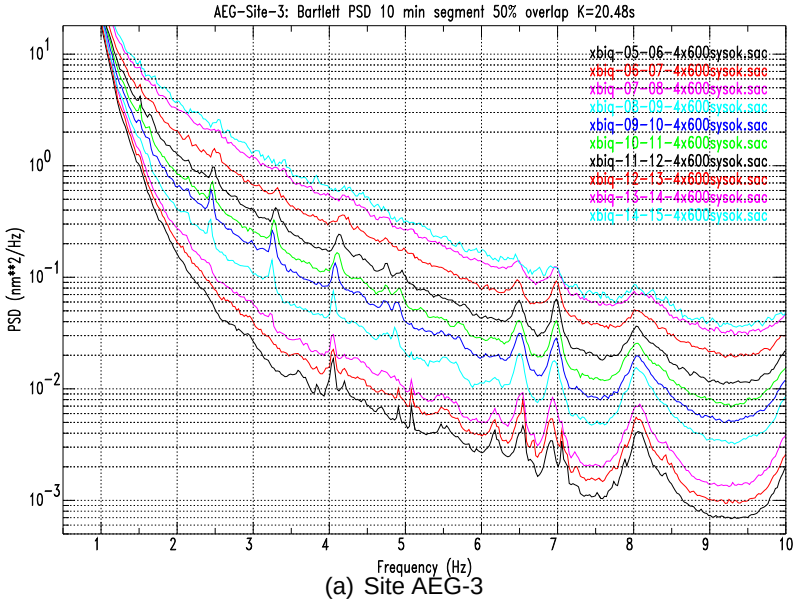

(a) Site AEG-3

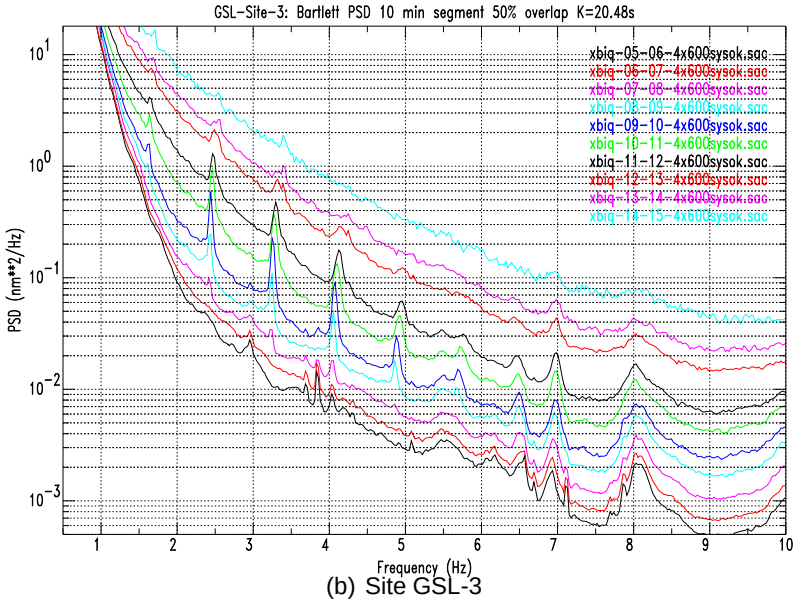

(b) Site GSL-3

Figure 6: Inter-quartile mean vertical displacement PSD from two of the sites that seem to be susceptible to wind-generated ambient background noise, (a) AEG-3, and (b) GSL-3, for a range of wind speeds in bins of 1m/s when all four turbines at Craig are generating electricity.

The linear inter-quartile mean PSD plots from all eight sites with wind speed are in Appendix A, and the corresponding logarithmic plots are in Appendix B. Two of sites (GSL-2 and AEG-4) seem to be dominated by broadband ambient background noise and show no clear harmonic peaks characteristic of the SGV from wind turbines.

4.4 Possible bias due to ambient background noise

The ambient background seismic noise at EKA depends partly on the wind velocity (see Figure 7, plots EKA array averaged rms SGV against wind speed data from a 50m high tower on Ewesdown Fell about 1.75km to the southeast of the “red 10” seismometer at EKA, operated by RDC during 2002). The threshold of 0.336nm used to safeguard EKA (Styles *et al.* 2005) was measured in the 1.5-4.5Hz passband, and was based on one month of hourly averaged wind speed data from an anemometer at a height of 10 m at the meteorological station in the valley at Eskdalemuir. Figure 7 gives the results of a much more detailed study by AWE of seven months of data and shows that the threshold of 0.336nm corresponds to a wind speed at 50m height of around 6m/s at EKA.

Analysis of the vertical displacement PSDs from the eight sites at Craig suggests that some of the seismometers deployed in the field, using the method described by Brisbourne *et al.* (2011), are more sensitive to strong winds than for observatory deployment, such as at EKA. Figure 8 shows the vertical displacement rms SGV values, calculated by integrating the inter-quartile mean PSD in the 1.5-4.5Hz passband and taking the square-root, with wind speed for seven of the sites analysed at Craig (GSL-2 is discarded due to what are presumed site installation problems). At low wind speeds the rms SGV values are about a factor of two above those at EKA (Figure 7). However, as the wind speed increases so the rms values increase non-linearly for all but the quietest sites at AEG-2b and AEG-5, where a linear relationship seems to hold, at least up to wind speeds around 15m/s.

The displacement PSDs from AEG-2b and AEG-5 are those dominated by power in the harmonic spectral peaks in the 1.5-4.5Hz passband, characteristic of the SGV from wind turbines. Notably, sites AEG-2b and AEG-5 are in a valley, and are largely sheltered from the strongest of the winds, whereas the other sites are on upland sites exposed to the wind. We suspect that as the wind increases, the whole soil layer at the temporary upland sites (where seismometer emplacement is in a hole back-filled with sand) starts to vibrate, and this manifests itself as broadband ambient background noise dominating the wind turbine SGV signal in the PSDs. Thus, in the following we tend to focus on

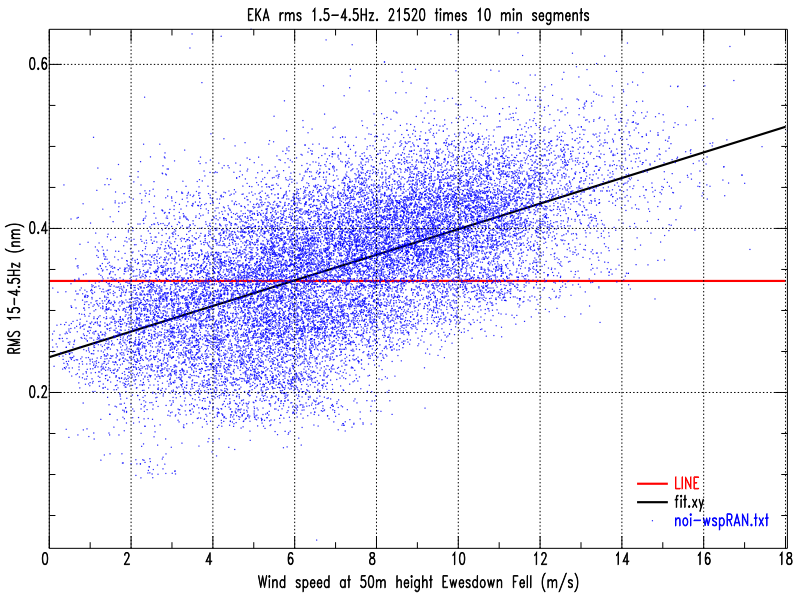

Figure 7: EKA ambient background noise in the 1.5-4.5Hz passband with wind speed at a height of 50m. Linear regression with errors in x and y: $y = 0.243 + 0.0156\,x$. The red line indicates the threshold of 0.336nm.

the data from sites AEG-2b and AEG-5. Separation of turbine SGV signal from ambient background noise is a research area identified in Stage One of the technical proposal agreed by the EWG (EWG 2012a)[2].

5 Preliminary evaluation of the source-term

5.1 Comparison of measured SGV with model predictions

For wind speeds above 8m/s the vertical displacement PSDs from AEG-2b and AEG-5 are dominated by power in the harmonic spectral peaks in the 1.5-4.5Hz passband, characteristic of the SGV from wind turbines. Since the threshold was originally defined in the 1.5-4.5Hz passband (Styles *et al.* 2005), it seems natural to initially focus on the AEG-2b and AEG-5 PSDs in this passband where turbine generated SGV power dominates, i.e., where the signal-to-noise ratio (SNR) is highest.

Table 4 gives the rms SGV (in nm), calculated by integrating the inter-quartile mean

[2]One test of the effectiveness of a turbine signal and ambient noise power separation scheme could be that the resulting estimated turbine SGV versus wind speed relationship should be similar at all sites where turbine signals are seen.

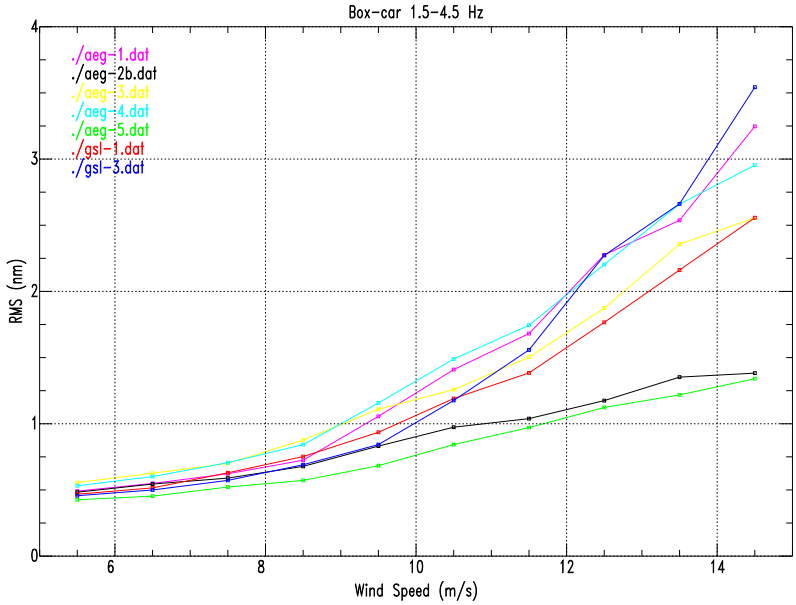

Figure 8: Vertical displacement rms SGV values, calculated by integrating the inter-quartile mean PSD in the 1.5-4.5Hz passband, with wind speed for seven of the sites analysed at Craig.

vertical displacement PSD in the 1.5-4.5Hz passband, and taking the square-root, for a range of wind speeds where characteristic turbine SGV dominates the PSDs. Interestingly the turbine generated rms SGV is strongly linearly related to the wind speed with Pearson correlation coefficients (Press *et al.*, 1992) of 0.992 and 0.998 for AEG-2b and AEG-5 respectively.

Table 4 also gives the cumulative SGV predicted by the Styles 2005 model, assuming that all four turbines are operating at 2.5MW output (i.e., with no 60% “utilisation” factor), and using the distances given in Table 1. It is clear that the measured rms SGV is significantly less than that predicted, by at least a factor of six, and can be around an order of magnitude smaller. However, the frequency of the dominant SGV power peak from the Craig pitch-regulated wind turbines is around 1.7Hz (see Figure 5).

5.2 A hypothetical source-term approximated at 1.7Hz?

Figure 9 shows the relative attenuation with distance of a source-term of strength unity at 1km with a narrow-frequency approximation of 4.5Hz, as in the 2005 model, and a hypothetical source-term a tenth of the size, but approximated at a frequency of 1.7Hz.

Site	2005 model prediction (nm)	Wind speed range (m/s) 8-9	9-10	10-11	11-12	12-13	13-14	14-15
AEG-2b	11.375	0.678	0.831	0.974	1.039	1.175	1.353	1.382
(ratio)	1.00	16.8	13.7	11.7	10.9	9.68	8.41	8.23
AEG-5	8.694	0.572	0.683	0.843	0.971	1.123	1.218	1.341
(ratio)	1.00	15.2	12.7	10.3	8.95	7.74	7.14	6.48

Table 4: rms SGV (in nm), calculated by integrating the inter-quartile mean vertical displacement PSD in the 1.5-4.5Hz passband, and taking the square-root, for a range of wind speeds where characteristic turbine SGV dominates the PSDs. Also listed is predicted rms SGV from the 2005 model, and the ratio of the predicted to the measured rms SGV.

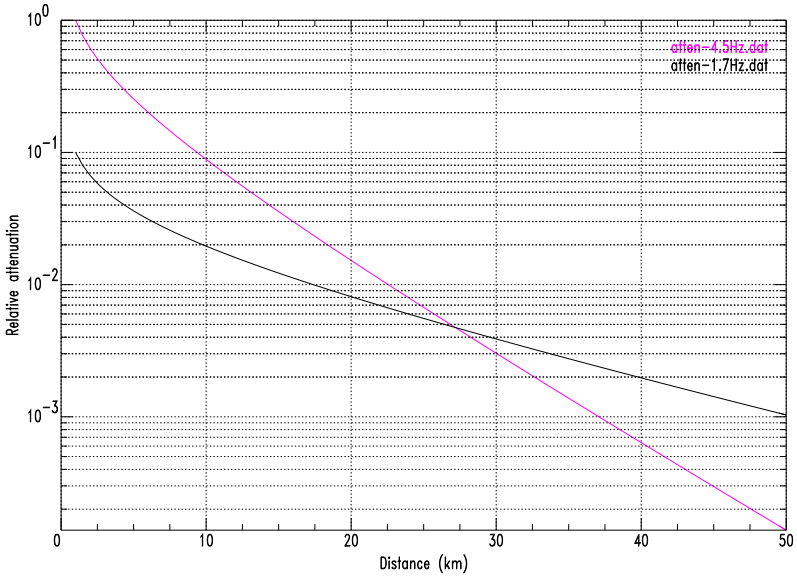

Figure 9: Relative attenuation with distance of a source-term of strength unity at 1km for a narrow-frequency approximation at 4.5Hz, as in the 2005 model (magenta line), and a hypothetical source-term a tenth of the size, but approximated at a frequency of 1.7Hz (black line).

It is clear that the relative contribution to the cumulative predicted SGV at EKA for a given turbine is greater using the 2005 model than the hypothetical term, out to a distance of around 27km; beyond 27km the 2005 model predictions are less than for the smaller hypothetical source-term at a frequency of 1.7Hz. In terms of area for potential wind farm development in the consultation zone around EKA, there is around 2000km^2 in the annulus between radii of 10 and 27km, compared with an annulus with area of some 5500km^2 between radii of 27 and 50km.

If we consider the narrow-frequency approximation in the 2005 model with a hypothetical source-term reduced by a factor of 10, and instead of using 4.5Hz we use 1.7Hz, then for wind farms spatially distributed similarly to those currently not objected to by MOD in the consultation zone, the hypothetical cumulative predicted SGV is about 75% of the threshold. For a hypothetical 1.7Hz source-term reduced by a factor of around seven, then the cumulative predicted SGV is roughly equal the threshold (as is the case at the time of writing with the threshold being reached using the 2005 model).

To some extent then the analysis above based on the Craig measurements and the narrow-frequency approximation may suggest prospects for “headroom” to accommodate further large wind turbine development in the consultation zone. However, Figure 9 shows that a hypothetical model based on a narrow-frequency around 1.7Hz would not penalise development close to EKA as strongly as the 2005 model. Furthermore, the area of the annulus defined from 27 to 50km is roughly 2.5 times greater than the annulus defined from 10 to 27km — this requires consideration given objective 2 of the EWG “to maximise MW and protect the array” (EWG 2012b).

The picture of how to proceed with re-examining the source-term is complicated by the blade-pass frequency from pitch-regulated MW-class turbines, which is less (around 0.85Hz) than for the stall-regulated turbines such as at Dun Law (around 1.4Hz). Thus, the SGV from MW-class pitch-regulated turbines has more harmonic peaks in the 0.5-8.0Hz passband of interest than the SGV from stall-regulated turbines. There are three significant spectral peaks less than 4Hz from the Craig pitch-regulated turbines (see Figure 4), compared to just one around 2.8Hz for the stall-regulated turbines at Dun Law (see the red line in the displacement PSD in Figure 1).

Thus, a hypothetical narrow-frequency approximation at 1.7Hz does not tell the whole story, as the effective source-term from pitch-regulated turbines is a broadband spectrum, the high-frequencies of which are increasingly attenuated with increasing distance. So the SGV spectrum at EKA from wind turbines at the outer reaches of the consultation zone will be dominated by low-frequency power compared with the SGV spectrum

at shorter distances. We also know that the displacement noise spectrum at EKA is strongly red-shifted — compared with other global seismometer arrays, at frequencies less that around 2Hz EKA is noisy, but at frequencies above 2Hz EKA is a quiet site. To account for all these and other factors in a quantitative way we need to develop appropriate frequency weighting.

6 Frequency-dependent weighting

Here we develop a method to quantify the impact of wind turbine generated SGV on the ability of EKA to detect seismic signals from underground nuclear explosions. The work described in this section relies heavily on a scientific paper in preparation by Selby and Bowers (2013). Since the SGV power and detection capability vary with frequency, our approach is to develop an objective physics-based frequency-weighting function, which can be used to calculate the effective (i.e. weighted) SGV power at EKA from a wind turbine at a given distance. The method presented here does not depend on the form of the SGV, other than that it can be represented by a power spectrum generated at the site of the turbine — the “source term”.

The frequency weighting to the broadband source-term PSD proposed is based on the optimal frequency filter for signal detection at EKA (Selby 2008), that depends only on physical properties at EKA, (1) the EKA ambient background vibration noise spectrum at windy times, (2) the signals expected at EKA from putative underground nuclear explosions under the CTBT, and (3) a term to account for the low-pass filter effect of signal processing (beamforming) at EKA, due to the increasing sensitivity of signals from long range to near-receiver effects with increasing frequency (for example, topographic effects local to individual seismometers at EKA).

The resulting weighting function depends on frequency and distance, and requires a calibration or normalisation factor that depends on its application. For the purposes of this interim report the application of the weighting function is in relation to the observed SGV from MW-class turbines relative to the threshold, which was calculated in the 1.5-4.5Hz passband. It should be noted that the “finalised” weighting function, ultimately used in the substantive Stage One research to quantify any “headroom” to accommodate further wind farm development in the consultation zone, could be for a different application to that considered here (for example, a revised definition of the threshold), and thus may require a different calibration.

6.1 Weighting theory

Application of the frequency weighting function, $F(f)$ to the source-term PSD, $T(f, r_{\text{ref}})$, for single operating turbine defined at a reference distance, r_{ref}, will give the frequency-weighted or effective source-term spectrum, $T(f,\ r_{\text{ref}})\,\gamma_0^2\,F(f)$.

The effective SGV power at EKA due to a single operating wind turbine at distance r is then $\gamma^2(r)$, with,

$$\gamma^2(r) = \gamma_0^2 \int_{f_1}^{f_2} F(f)\ T(f, r_{\text{ref}})\, P(f, r, r_{\text{ref}})\, df, \tag{1}$$

where f is frequency in Hz, with the integration over the passband f_1 to f_2 Hz (for example, the 0.5-8.0Hz teleseismic band for which signals from underground nuclear explosions may be detected Bache *et al.*, 1985).

$P(f, r, r_{\text{ref}})$, is the propagation term from r_{ref}, and accounts for geometrical spreading and the frequency dependent effects of attenuation, with,

$$P(f, r, r_{\text{ref}}) = \left[\left(\frac{r}{r_{\text{ref}}} \right)^{-\frac{1}{2}} \exp\left(\frac{-\pi\ f\ (r - r_{\text{ref}})}{Q\ v} \right) \right]^2, \tag{2}$$

where Q is the apparent attenuation factor and v the group speed, with the turbine-generated SGV propagating as a surface wave, and $F(f)$ is the optimal signal detection filter at EKA. γ_0^2 is a normalisation or calibration factor.

We construct $F(f)$ using the background noise power spectrum, $N^2(f)$, and the power spectrum of "signals of interest", typically teleseismic signals from underground nuclear explosions recorded at EKA, $S^2(f)$. To derive the form of $F(f)$, we start with the familiar Wiener filter, $W(f)$, which produces a signal estimate closest to the true signal in a least-squares sense,

$$W(f) = \frac{S^2(f)}{S^2(f) + N^2(f)}. \tag{3}$$

The variance of the Wiener estimate is,

$$\sigma_W^2 = \frac{S^2(f)N^2(f)}{S^2(f) + N^2(f)}, \tag{4}$$

which can be demonstrated by calculating the squared difference between the true signal and Wiener-filtered signal plus noise. The optimal signal detection filter, which optimises detection while reducing false alarms, is the Freiberger filter (Freiberger 1963). As the weighting is to be applied to power spectra we use the squared Freiberger filter, $F(f)$,

which is the squared Wiener filter divided by its variance, i.e.,

$$\begin{aligned} F(f) &= \frac{W^2(f)}{\sigma_W^2(f)}, \\ &= \frac{1}{N^2(f)} \frac{S^2(f)}{S^2(f) + N^2(f)}. \end{aligned} \tag{5}$$

For large signal-to-noise ratio (SNR), $F(f) \simeq 1/N^2(f)$, i.e., the effect is a whitening of the noise power spectrum. For example, this would indicate that for turbine-generated SGV of constant power with frequency, the impact is greater where the background noise is lower. For lower SNR, the effect of $F(f)$ is to whiten the background noise and then apply a filter $S^2(f)/(S^2(f) + N^2(f))$, which emphasises the frequency band in which the expected signal power is strongest. We now explore in detail the expected form of the signal and noise power spectra, $S^2(f)$ and $N^2(f)$.

6.1.1 Teleseismic signal model

We use a simple model of the observed signal power spectrum, $S^2(f)$, suitable for teleseismic signals from both earthquakes and underground (chemical and nuclear) explosions,

$$S^2(f) = \zeta^2 \; C^2(f) \; B(f) \, |e^{-\pi \; t^* \; f}|^2, \tag{6}$$

where ζ^2 is a scaling factor dependent on the absolute size of the signal, and $C(f)$ is the source spectrum, defined by,

$$C(f) = \begin{cases} 1, & f \leq f_c \\ f^{-2}, & f > f_c, \end{cases} \tag{7}$$

where f_c is the corner frequency. Since the primary events of interest under the CTBT are likely to be small, deep explosions, we assume $f_c > 8$Hz, and so $C(f) = 1$ within the 0.5-8Hz frequency band of interest. The parameter t^* is the apparent P wave attenuation for teleseismic signals. $B(f)$ is the beam coherency, the ratio of the signal power on the beam to the average of the K individual channels, i.e. the *semblance* (Neidell and Taner, 1971). This describes how beamforming acts as a low-pass filter (because signal correlation across the array tends to decrease with increasing frequency). We choose

$B(f)$ to be of the form,

$$B(f) = \begin{cases} \frac{1}{K}\left[1 + \frac{K-1}{2}\left(1 + \cos\left[\frac{\pi f}{f_{\mathrm{MAX}}}\right]\right)\right], & f \leq f_{\mathrm{MAX}} \\ \frac{1}{K}, & f > f_{\mathrm{MAX}} \end{cases} \tag{8}$$

where f_{MAX}, to be determined, is the maximum frequency at which beamforming improves the SNR (above this frequency the signal is uncorrelated between channels of the array, and so beamforming reduces the power of the signal to $1/K$ of the power on a single channel, the same factor as for random uncorrelated noise).

Rather than choose an absolute value of ζ^2 to scale the source spectrum, we assume a reasonable minimum detectable SNR of two. Consequently, once the shape of $S^2(f)$ and $N^2(f)$ have been determined, we choose ζ^2 such that,

$$\left.\frac{S^2(f)}{N^2(f)}\right|_{\mathrm{max}} = 4. \tag{9}$$

6.1.2 Noise model

The power of background seismic noise generally rapidly decreases with increasing frequency, and this decrease is particularly pronounced at stations near continental margins such as EKA. We model the PSD of the background noise, $N^2(f)$, on a single channel, with a function of the form,

$$\log_{10}[N^2(f)] = A_0 + A_1 \log_{10} f + A_2 \log_{10}^2 f, \tag{10}$$

where A_0, A_1 and A_2 are to be determined.

6.2 Normalisation

Here we consider the γ_0^2 term for the normalisation or calibration of $F(f)$. The γ_0^2 term is required to get an interpretable value for the output of the integration in equation 1, because the Freiberger filter (unlike the Wiener filter) is dimensioned because of the $1/N^2(f)$ term. The approach taken to determining an appropriate γ_0^2 could depend on the form of the source-term, $T(f, r_{\mathrm{ref}})$.

For example, in the 2005 model the source-term is based on a narrow-frequency approximation at a frequency of 4.5Hz. Thus, it might seem intuitively attractive for applications

involving the 2005 model for, $\gamma_0^2\, F(f)|_{f=4.5} = 1$.

Clearly, the there are multiple spectral peaks, in the 0.5-8Hz passband of interest for the detection of signals from underground nuclear-explosions, at harmonics of the blade-pass frequency from the Craig pitch-regulated turbines (see Figure 4). Thus, a model of the source-term based on the narrow-frequency approximation is not appropriate.

The aim of the initial study is to provide the EWG with information to determine whether it is worth pursuing Stage One — the substantive research stage to re-examine the 2005 model (Objective 1 of the EWG; EWG 2012b). To achieve this the technical proposal to the EWG (EWG 2012a) has as key outputs from the initial study a comparison with the SGV predicted by the 2005 model, and an assessment of whether there are prospects for "headroom" to accommodate further large wind turbine development in the consultation zone. For the initial study the "headroom" is with reference to the threshold of 0.336nm used by MOD to safeguard EKA. Since the threshold was calculated in the 1.5-4.5Hz passband it is this passband that is taken as appropriate for the definition of the γ_0^2 term for normalisation of $F(f)$ *for the initial study*.

It seems intuitive that the γ_0^2 term should be chosen such that normalised $F(f)$ should have the same power as the filter (with weights of unity between low and high cut-off frequencies) used to to calculate the threshold. This definition is consistent with the original calculation of the threshold, and is expressed as,

$$\gamma_0^2 \int_{f_1}^{f_2} F(f)\, df = f_2 - f_1, \tag{11}$$

where, for the initial study $f_1 = 1.5$Hz and $f_2 = 4.5$Hz. For the 11-12m/s wind speed bin noise model (see Section 6.3.2), used later, and other measured parameters this is equivalent to normalising $F(f)$ to unity at $f \approx 3.28$Hz, such that $\gamma_0^2 F(f)|_{f\approx 3.28} = 1$.

6.3 Measurement of required parameters for weighting

Having developed the theoretical aspects of equation(1), we require values for seven parameters, shown in Table 5, to determine the exact form of $F(f)$ and $P(f, r, r_{\text{ref}})$.

The value for Q, the quality factor (attenuation) for surface waves propagating in the Southern Uplands of Scotland, is that used by Styles *et al.* (2005) and is taken from MacBeth and Burton (1987). A value for $t^* = 0.15$s, the attenuation of teleseismic P waves, is found in Bache *et al.* (1985) and Stewart (1988). To avoid confusion, this is

Parameter	Value	Description	Source
v	2km/s	Group speed	Styles *et al.* (2005)
Q	50	Apparent attenuation factor	MacBeth and Burton (1987) Styles *et al.* (2005)
t^*	0.15s	Attenuation of teleseismic body waves	Bache *et al.* (1985) Stewart (1988).
f_{MAX}	6.5Hz		§6.3.1
A_0	1.11	11-12m/s bin	§6.3.2
A_1	-8.78		§6.3.2
A_2	3.96		§6.3.2

Table 5: Source of parameters used in this interim report.

the value for the so-called "apparent" t^* in the short-period band. Next we explore beam coherency and background noise spectra at EKA.

6.3.1 Beam coherency

The beam coherency or semblance, $B(f)$, describes how beamforming acts as a low pass filter, as the similarity of signals recorded at elements of the array decreases with increasing frequency. Earlier we assumed the form of a function to describe $B(f)$, and in this section we summarise an investigation into a reasonable value for the parameter f_{MAX}, based on measurements from observations of earthquake and explosion signals.

We select all earthquakes with body-wave magnitude, $m_{\mathrm{b}} \geq 5.5$ from the Reviewed Event Bulletin (REB) of the International Data Centre (IDC) in the period 2009-2011. This gives a total of 120 earthquakes. We require an SNR of at least 10 on each of the 20 individual channels of the array. This is to ensure that the semblance measure is not degraded by background noise. This criteria reduces the number of usable earthquakes to 61.

The semblance is calculated for 50 overlapping frequency-filter bands (a Hanning window with a width of 1Hz) between 0.25 and 8.5Hz. As expected the semblance clearly reduces with increasing frequency, although the observations are scattered. We fit a function of the form indicated by equation 8 by minimising the absolute-value misfit. We find $f_{\mathrm{MAX}} = 6.5$Hz.

We compare these results with observations from underground nuclear explosions at two former test sites — 7 and 13 explosions at the Novaya Zemlya (in the Russian Arctic) and Degelen (in east Kazakhstan) respectively. The measurements from Novaya Zemlya

and Degelen are in good agreement with the model fit derived from the earthquake observations.

6.3.2 Noise model

We explore the relationship between the ambient background seismic noise at the EKA array and wind speed. We make use of wind speed observations from a temporary anemometer deployment during seven months of 2002 at Ewesdown Fell about 1.75km to the southeast of the “red 10” element of EKA. The wind speed is recorded at a height of 50m and the average wind speed is given every 10 minutes.

For each 10 minute segment we retrieve the seismic waveforms recorded at EKA from the data archive at the UK National Data Centre (at AWE Blacknest). As a quality control we measure the rms of each waveform and the maximum amplitude. Channels with peak amplitude more than six times the rms are excluded (as this is a good indicator of the presence of signals or noise spikes which would distort the observation of the background noise power spectrum).

Power spectra are then calculated and grouped by wind speed bin. The median spectra is found for each group and a curve is fit to calculate A_0, A_1, A_2 (equation 10). The results are given in Table 6. The noise power spectra are approximately the same shape for all wind speeds, the main effect being a shift in the absolute level of the noise.

6.4 Frequency and distance weighting

6.4.1 Effective source-term frequency weighting

Figure 10 shows the frequency-weights for the effective source-term spectrum, $\gamma_0^2 F(f)$ in equation(1). The black curve is for $\gamma_0^2 F(f)$ calculated using the noise model corresponding to the mode of the wind speed (5-6m/s bin) in Table 6. The red line is $\gamma_0^2 F(f)$ for the noise model corresponding to the 11-12m/s wind speed bin (see Table 6). It is clear that the shape of the resulting $\gamma_0^2 F(f)$ curves are only weakly dependent on the noise model chosen. In the following analysis the noise model corresponding to the 11-12m/s wind speed bin has been used (see Table 5). The peak of the filter is around 5Hz. This is perhaps a counter-intuitive result for seismologists, but is because of the “extra” $1/N^2(f)$ term in the definition of $F(f)$.

Wind speed (m/s)	N	A_0	A_1	A_2
0-1	207	0.61	-7.96	3.49
1-2	808	0.64	-7.79	3.36
2-3	1500	0.66	-7.79	3.36
3-4	1962	0.71	-8.07	3.52
4-5	2398	0.75	-8.24	3.61
5-6	2901	0.80	-8.35	3.64
6-7	2885	0.85	-8.33	3.61
7-8	2734	0.93	-8.45	3.68
8-9	2559	1.00	-8.58	3.76
9-10	2332	1.06	-8.73	3.86
10-11	1943	1.08	-8.72	3.87
11-12	1348	1.11	-8.78	3.96
12-13	687	1.13	-8.65	3.91
13-14	372	1.15	-8.62	3.94
14-15	232	1.19	-8.67	4.09
15+	185	1.22	-8.85	4.32

Table 6: Distribution of wind speed and corresponding least-squares fit estimates of the parameters A_0, A_1, A_2 (equation 10).

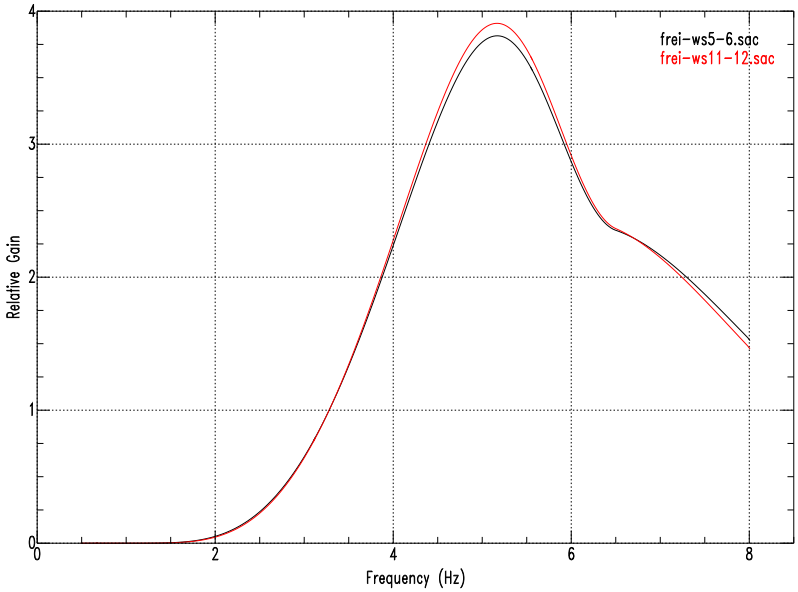

Figure 10: The black and red curves are the filters $\gamma_0^2 F(f)$, calculated using the noise models, corresponding to the 5-6m/s and 11-12m/s wind speed bins respectively.

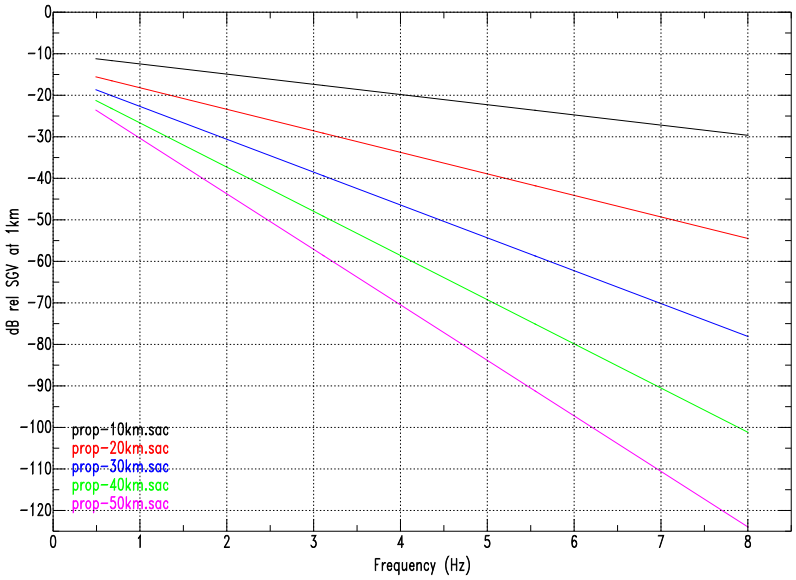

Figure 11: Frequency-dependence of the propagation term $P(f, r, r_{\text{ref}})$ in equation(1) in dB for a range of distances to EKA. 10km (black), 20km (red), 30km (blue), 40km (green), 50km (magenta), with $r_{\text{ref}} = 1$km.

6.4.2 Propagation-term frequency and distance weighting

Figure 11 shows the frequency-dependence of the SGV propagation term, $P(f, r, r_{\text{ref}})$ (equation 2) for distances to EKA, r = 10, 20, 30, 40 and 50km, with $r_{\text{ref}} = 1$km. The figure demonstrates clearly the strong effect propagation has on the predicted SGV from a wind turbine at EKA. For example, at 4Hz the SGV at 50km distance is 50dB smaller than that at 10km (a factor of over 300 in amplitude). At 2Hz the SGV at 50km is 30dB smaller than at 10km (a factor of about 30 in amplitude).

6.4.3 Combined frequency and distance weighting

Examples of the combined frequency and distance weighting terms, $w(f, r, r_{\text{ref}})$,

$$w(f, r, r_{\text{ref}}) = \gamma_0^2 \, F(f) \, P(f, r, r_{\text{ref}}), \tag{12}$$

to be applied to the single operating turbine source term PSD, $T(f, r_{\text{ref}})$ in equation(1), for a range of distances are shown in Figure 12. Table 7 lists the gain at the peak, and corresponding frequency, of the filter for the distances shown in Figure 12. As well as the peak gain reducing rapidly with distance, the frequency of the peak gain moves

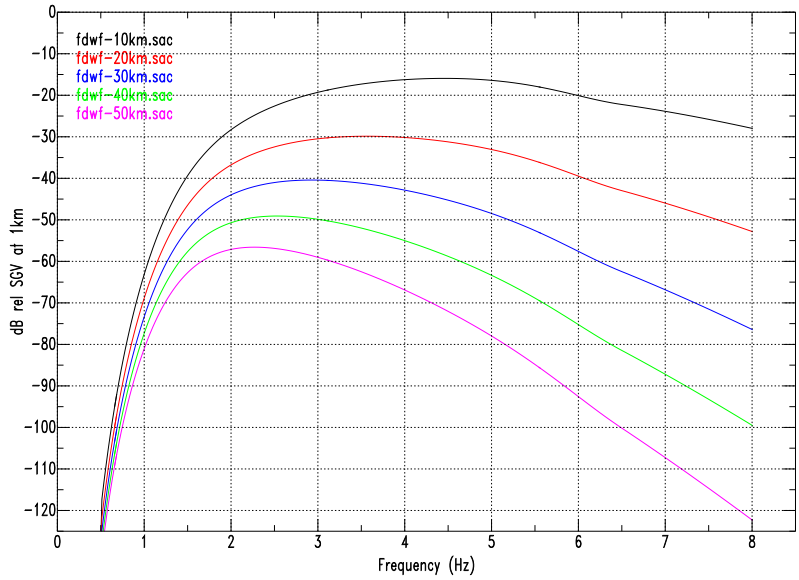

Figure 12: Combined frequency and distance weighting terms (in dB), to be applied to the source term PSD in equation(1) for a range of distances. 10km (black), 20km (red), 30km (blue), 40km (green), 50km (magenta), with $r_{\text{ref}} = 1$km.

progressively to lower frequencies with increasing distance. Table 7 also shows the frequencies of the "$-$3dB point" (also commonly referred to as the "cut-off frequency" or the "half-power point"), which corresponds to the frequencies at which the gain of the combined frequency and distance weight filter is half the peak gain. The difference in the $-$3dB points is taken as a measure of the passband of the filter — the passband of the combined frequency and distances weighting filter reduces with increasing distance.

7 Preliminary estimates of the source-term — 0.5-8.0Hz pass-band

7.1 Data selection

Figure 13 compares the inter-quartile mean PSD calculated for the 11-12m/s wind speed bin at sites AEG-2b and AEG-5, for when all four turbines at Craig wind farm are operating. The 11-12m/s wind speed bin is selected as the Nordex N-80 turbine is operating at approaching rated-power, and the number of 10-minute segments used to estimate the inter-quartile mean PSD starts to fall-off sharply for greater wind speeds (see Table 3. The PSDs in Figure 13 are remarkably similar in shape and in absolute power across

Distance	10km	20km	30km	40km	50km
Peak filter gain	2.548E-02	1.031E-03	9.072E-05	1.234E-05	2.194E-06
Peak frequency	4.47Hz	3.56Hz	2.93Hz	2.54Hz	2.27Hz
−3dB peak (low f)	3.08Hz	2.44Hz	2.08Hz	1.86Hz	1.71Hz
−3dB peak (high f)	5.76Hz	4.96Hz	4.13Hz	3.52Hz	3.08Hz
“Passband”	2.69Hz	2.51Hz	2.05Hz	1.66Hz	1.37Hz

Table 7: Gain at the peak, and corresponding frequency, of the combined frequency and distance weighting filter at the distances shown in Figure 12. Also given are the frequencies corresponding to −3dB of the peak gain, and the difference between them (referred to here as the “Passband”).

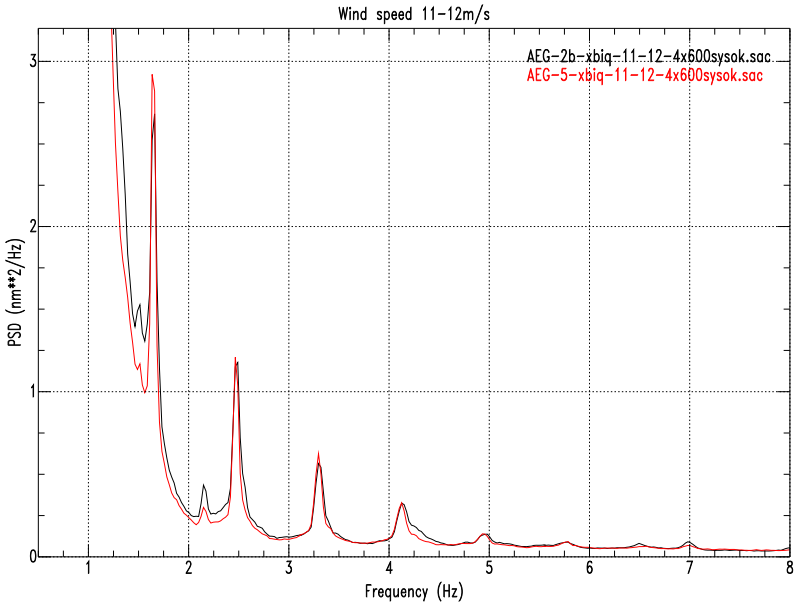

Figure 13: Comparison of the inter-quartile mean PSD calculated for the 11-12m/s wind speed bin at sites AEG-2b (black) and AEG-5 (red). These are denoted $T'_k(f)$ in equation(13)

the frequency range 0.5-8Hz, except for the clear, but small spectral peak around 2.15Hz where the SGV power at site AEG-5 is about half that at site AEG-2b.

The two sites are in different directions from the four wind turbines (see Figure 2) with AEG-2b (instrument 6099) to the northwest, and AEG-5 (instrument 6351) to the north, of turbine 2 at Craig wind farm. In addition to the differing directions from the wind turbines the two sites are also at different distances, with sites AEG-2b and AEG-5 being 595m and 1084m from turbine 2, respectively. Given the distance dependence of the propagation term in equation(2) we might expect different weighting for the PSDs calculated from data recorded at sites AEG-2b and AEG-5.

7.2 Frequency-distance weighting for SGV from multiple turbines

The combined frequency and distance weighting filter in equation(12) is for a single operating turbine. The SGV PSD from the 2011 Craig spectra with the highest SNR are from sites AEG-2b and AEG-5 (Figure 5), and are for when all four 2.5MW pitch-regulated turbines are operating. To compare the rms SGV from the calculated PSD at the kth site from the data, $T'_k(f)$ (examples are shown in Figure 13) with that predicted by the 2005 model for a range of distances requires a frequency-distance correction as the seismometers sites were not at a common reference distance from all four of the Craig turbines (see Table 1).

If we assume that the phase of the turbine blade passing the tower is a random process on average, then the weighted SGV PSD from each turbine sum linearly (as is assumed in the 2005 model). If we further assume, again as in the 2005 model, that each 2.5MW turbine at Craig generates the same amount of SGV at a given (reference) distance (i.e., we assume that directional effects are either negligible or cancel), then the rms at distance r, is the square-root of, $\Gamma^2_k(r)$ from all four operating turbines at Craig (with distances from each N turbines to the kth site, r_{jk}, $j = 1, N$) where,

$$\Gamma^2_k(r) = \int_{f_1}^{f_2} T'_k(f)\, \frac{1}{N} \sum_{j=1}^{N} w(f, r, r_{jk})\, df. \tag{13}$$

Figure 14 compares the frequency weights from equation(13) to simulate the SGV at a distance of 20km from the four turbines operating at Craig, using the SGV PSD calculated from the data recorded at the AEG-2b and AEG-5 sites. The weights were calculated using the distances to each of the four turbines given in Table 1. The relative

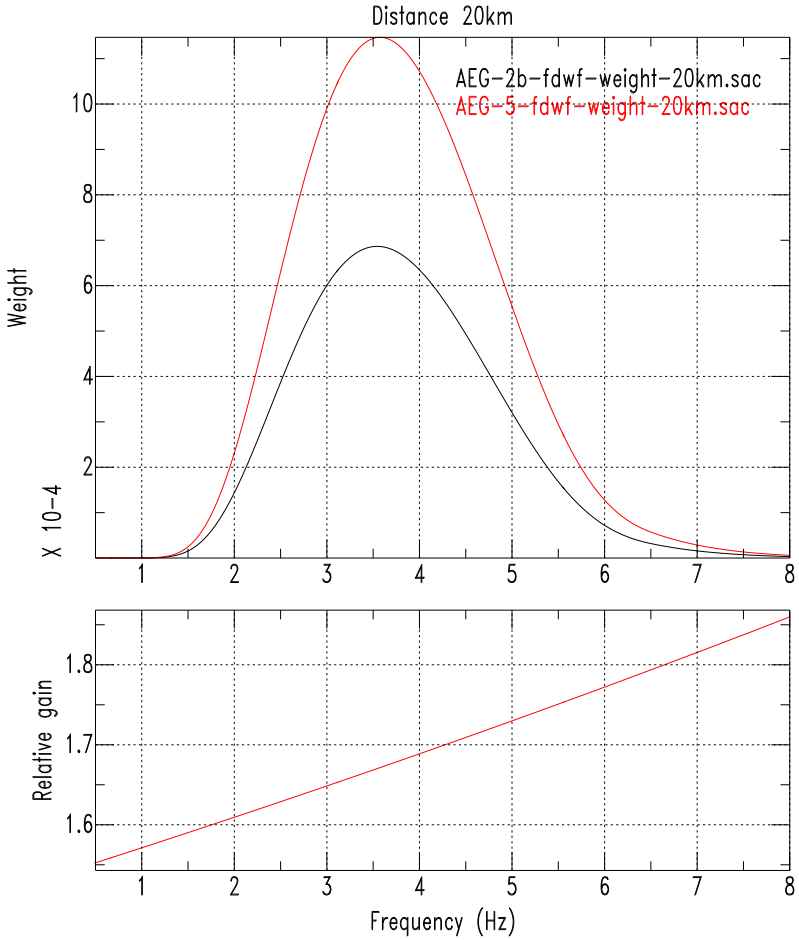

Figure 14: [Upper panel] Comparison of the frequency weights from equation(13) to simulate the SGV at a distance of 20km from the four turbines operating at Craig, using the SGV PSD calculated from the data recorded at the AEG-2b (black) and AEG-5 (red) sites. [Lower panel] The ratio of the AEG-5 weight to that for AEG-2b.

gain of the two weights is shown in the power panel of the figure, and shows a weak non-linear frequency dependence.

7.3 Comparison with 2005 model predicted SGV

Figure 15 compares the weighted inter-quartile mean PSD calculated for the 11-12m/s wind speed bin at sites AEG-2b and AEG-5. The weights are those from equation(13) for a distance of 20km shown in Figure 14. To obtain a preliminary estimate of the rms SGV value to compare with that predicted by the 2005 model, these curves are integrated, to

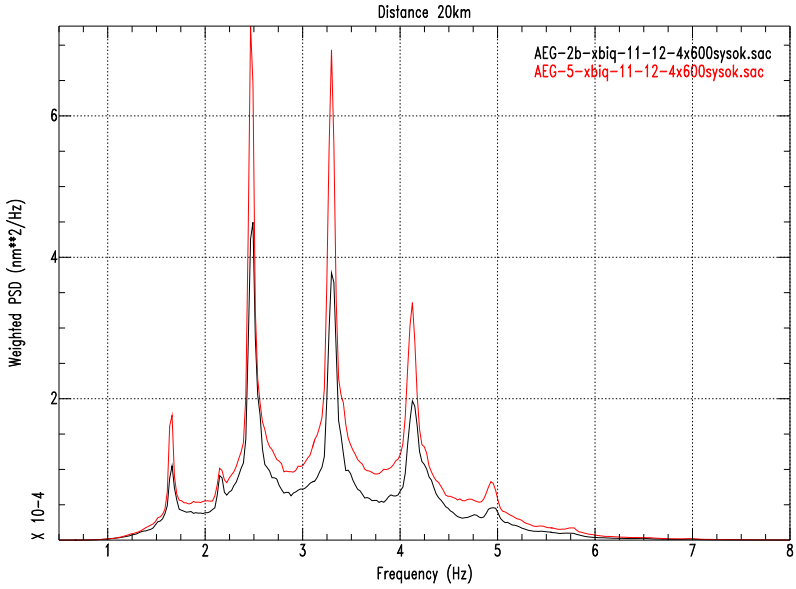

Figure 15: Comparison of the weighted inter-quartile mean PSD calculated for the 11-12m/s wind speed bin at sites AEG-2b (black) and AEG-5 (red). The weights are those from equation(13) for a distance of 20km shown in Figure 14

obtain the weighted SGV power in 0.5-8Hz passband, and then the square-root is taken. Figure 16 shows the weighted inter-quartile mean PSD calculated for the 11-12m/s wind speed bin at site AEG-5 for a range of distances to EKA.

Table 8 compares the rms SGV predicted by the Styles 2005 model at a range of distances within the consultation zone, and preliminary estimates of rms SGV from the weighted PSD calculated from data recorded at sites AEG-2b and AEG-5 for wind speeds in the range 11-12m/s. Also given is the ratio of the 2005 model prediction to the preliminary estimated rms SGV. This ratio can be thought of as the apparent overestimate of the source-term in the Styles 2005 model.

The size of the apparent overestimate depends on distance. Preliminary estimates of ratios, subject to independent validation and further research, are around eight at a distance of 10km, reducing to ratios around unity (i.e., no difference) at a distance of 50km. However, further consideration of possible bias due to direction and/or site effects, and other factors, such as the mode of SGV propagation, is required.

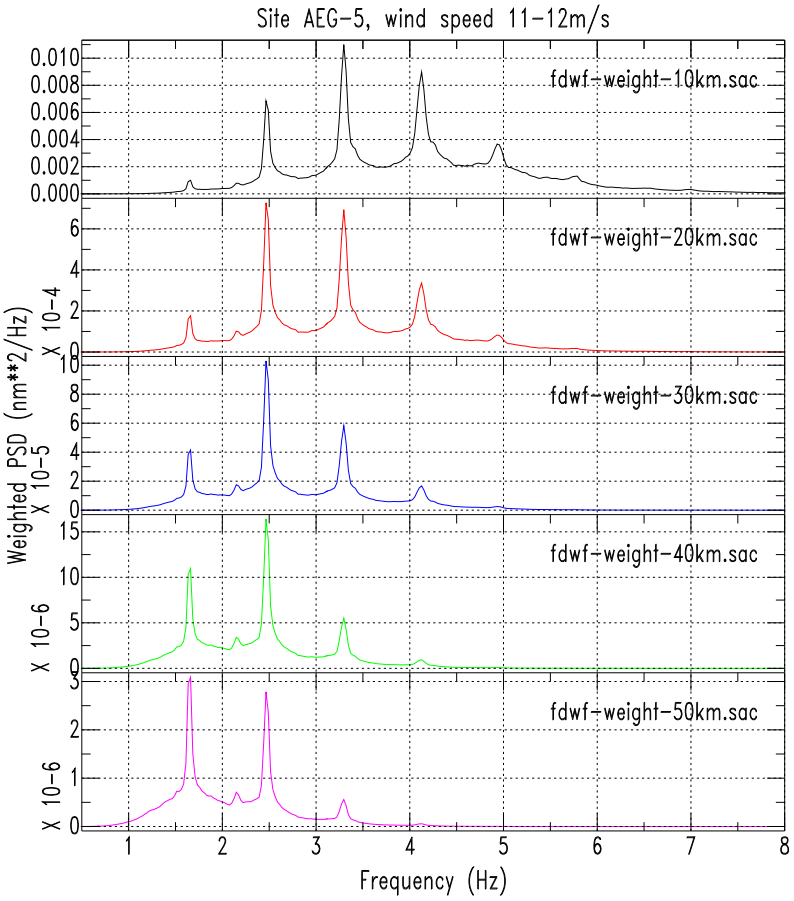

Figure 16: The weighted inter-quartile mean PSD calculated for the 11-12m/s wind speed bin at site AEG-5, for all four turbines at Craig operating, at a range of distances to EKA. 10km (black), 20km (red), 30km (blue), 40km (green), 50km (magenta).

Distance		10km	20km	30km	40km	50km
2005 model	rms (nm)	0.80645	0.13871	0.027547	0.0058028	0.0012625
AEG-2b	rms (nm)	0.079711	0.018159	0.0057997	0.0022627	0.0010096
	ratio	10.1	7.64	4.75	2.56	1.25
AEG-5	rms (nm)	0.099083	0.022205	0.0069726	0.0026795	0.0011817
	ratio	8.14	6.25	3.95	2.17	1.07

Table 8: Comparison of rms SGV predicted by the 2005 model at distances of 10km, 20km, 30km, 40km, and 50km, and preliminary estimates from the weighted PSD calculated from data recorded at sites AEG-2b and AEG-5 for wind speeds in the range 11-12m/s. Also given is the ratio of the 2005 model prediction to the preliminary estimated rms SGV.

8 Interim findings

8.1 Interim tentative conclusions

1. Far-field seismic data from eight sites in a field experiment at Craig wind farm in mid-2011 have been analysed. The seismometers were deployed at distances between 300m and 1500m from the four 2.5MW pitch-regulated turbines at Craig. Craig wind farm is in the consultation zone surrounding EKA. The 2005 model used to safeguard EKA is based on SGV data from stall-regulated turbines. The turbines so far constructed in the consultation zone are pitch-regulated turbines.

2. Statistical analysis of the displacement SGV PSD calculated from the vertical component, measured during the Craig experiment for a range of wind speeds when all four turbines are operating, demonstrates that the inter-quartile mean is a robust measure of the underlying SGV power spectrum.

3. Clear spectral peaks are identified in the PSD at integer multiples of the blade-passing frequency (around 0.85Hz) — this observation is diagnostic of SGV from operating wind turbines. The SGV PSD peak with the highest power is at a frequency around 1.7Hz, corresponding to the second multiple of the blade-pass frequency. The power in the spectral peaks at higher frequencies decreases with increasing blade-pass frequency multiple.

4. The frequency and power of each spectral peak, associated with multiples of the blade-pass frequency, increases with increasing wind speed. This strongly suggests that the dominant far-field SGV from pitch-regulated turbines is generated by the action of the turbine blades passing the tower, and not by excitation of structural vibration modes.

5. The two quietest sites, AEG-2b and AEG-5, were the most sheltered from the wind, and also have the SGV spectral peaks with the highest SNR. The rms SGV from these two sites measured in the 1.5-4.5Hz passband increases linearly with increasing wind speed, at least up to wind speeds around 15m/s. This linear relationship breaks down at the noisier sites, which were sited in upland/exposed areas, for wind speeds above around 7-8m/s.

6. MW-class pitch-regulated turbine blades rotate at a slower rate than stall-regulated turbines, and thus have a lower blade-pass frequency (around 0.85Hz and 1.4Hz

respectively). The passband for the detection of signals of interest by EKA under a CTBT is around 0.5-8Hz. Therefore the SGV from pitch-regulated turbines will have a larger number of more closely spaced spectral peaks at multiples of the blade-pass frequency in the passband of interest, than the SGV from stall-regulated turbines. Thus, a narrow-frequency approximation, as in the 2005 model, is not appropriate and frequency-distance weighting of the SGV PSD is required.

7. Relevant frequency-distance weighting theory has been developed based on optimal signal detection theory, and the physical properties of signals of interest and noise at EKA derived from observations. The propagation term in the frequency-distance weighting model uses the parameters adopted by Styles *et al.* (2005), i.e., that the far-field SGV from wind turbines propagates as surface-waves travelling at a group speed of 2km/s, with non-elastic attenuation characterised by an apparent $Q = 50$.

8.2 Interim preliminary results

1. For the purpose of this interim report the frequency-distance weighting developed is calibrated or normalised with respect to the 1.5-4.5Hz bandpass filter used to determine the threshold of 0.336nm. The threshold is used in the current MOD safeguarding approach (Styles *et al.* 2005).

2. The rms SGV predicted by the Styles 2005 model, at a range of distances within the consultation zone, is compared with preliminary estimates from the frequency-distance weighted SGV PSD calculated from data recorded at the two quietest sites during the Craig 2011 field experiment for wind speeds in the range 11-12m/s. The ratio of the 2005 model prediction to the preliminary estimated rms SGV can be thought of as the apparent overestimate of the source-term in the Styles 2005 model. The size of the apparent overestimate depends on the distance.

3. Preliminary estimates of ratios, subject to independent validation and further research, are around eight at a distance of 10km, reducing to ratios around unity (i.e., no difference) at a distance of 50km. However, further consideration of possible bias due to direction and/or site effects, and other factors, such as the mode of SGV propagation, is required.

4. Subject to validation by the FMB/EWG commissioned consultant (EWG 2012b) and further research, these interim preliminary results support the view that it is

likely to be worthwhile pursuing the substantive research into re-examination of the 2005 model, as envisaged in Stage One of the technical proposal (EWG 2012a), and with possible additional further work described below. The substantive research stage would quantify any “headroom” to accommodate further wind farm development in the consultation zone, and develop a mathematical model to be implemented in a software tool to enable effective safeguarding of EKA.

9 Further work

9.1 Initial study (with FMB/EWG commissioned consultant)

Further to the initial study key outputs outlined in the technical proposal (EWG 2012a):

1. Verify algorithms used in this interim report.
2. Validate the preliminary results presented in this interim report.
3. Consider directional and/or site effects.
4. Consider mode of propagation of SGV.

9.2 Stage One research

Further to the points described in Appendix A of EWG (2012a) the Stage One research could also consider:

1. Since far-field SGV is dominated by energy at frequencies that are integer multiples of the blade-pass frequency, and is not dominated by structural resonance modes, such as the second bending mode.
   (a) Investigate operational rotation rates of pitch-regulated MW-class turbines that are available now, and are in development. Identify physical constraints, such as blade-tip speed remaining sub-sonic.
   (b) Consider whether blade length, area, shape and pitch contribute to the far-field SGV.
   (c) Consider whether tower height, stiffness, and foundation conditions affect the far-field SGV generation.

(d) Consider implications for small wind turbines, especially three-bladed systems with rotation rates around 200rpm (equivalent to a blade-pass frequency around 10Hz). This may be as part of Stage 1B in the technical proposal agreed by the EWG (EWG 2012a).

2. Characterise the seismic wavefield contributing to the SGV, i.e., Rayleigh versus Love modes or a combination, by analysing the three-components of SGV.

3. Assess site effects and three-dimensional effects of geological structure and topography (e.g., focusing). Directional effects may be important. Development of a method of separating wind-turbine SGV from ambient background noise would be beneficial, as then the data from the "noisy" sites could be exploited, giving increased coverage over a wide range of directions.

References

Bache TC, Marshall PD, & Bache LB. 1985. *Q* for teleseismic *P* waves from central Asia. *J. Geophys. Res.*, **90**, 3575-3587.

Brisbourne A, Horleston A, Hawthorn D, & Lane V. 2011. SEIS-UK 6TD & ESPD Field Methods, Version 5.7, 24 March 2011.

EWG. 2012a. Technical proposal to the Eskdalemuir Working Group — Initial Study. 5 November 2012. http://www.scotland.gov.uk/Topics/Business-Industry/Energy/Infrastructure/Energy-Consents/Guidance (accessed 23 May 2013). 6pp.

EWG. 2012b. Notes from the Eskdalemuir Working Group meeting on 2 November 2012. http://www.scotland.gov.uk/Topics/Business-Industry/Energy/Infrastructure/Energy-Consents/-Guidance (accessed 23 May 2013). 7pp.

Fiori I, *et al.* 2009. A study of the seismic disturbance produced by the wind park near the gravity wave detector GEO-600. 3rd International Meeting on Wind Turbine Noise. Aalborg, Denmark. 25pp.

Freiberger WF. 1963. An approximate method of signal detection. *Q. Appl. Math.*. **20**, 373-378.

Neidell NS,& Taner MT, 1971. Semblance and other coherency measures for multichannel data. *Geophysics*, **36**, 482-497.

Peterson J. 1993. Observations and modeling of seismic background noise. USGS Open File Report, 93-322.

Press *et al.* 1992. Numerical recipes in Fortran. The art of scientific computing. Second edition. Cambridge University Press. 963pp.

Saccorotti G, Piccinini D, Cauchie L, & Fiori I. 2011. Seismic noise by wind farms: a case study from the Virgo Gravitational Wave Observatory, Italy. *Bull. Seismo. Soc. Am.*, **101**, 568-578.

Schofield R. 2001. Seismic measurements at the stateline wind project. Technical Report. LIGO-T020104-00-Z. 14pp.

Selby ND. 2008. Application of a generalised *F* detector at a seismometer array. *Bull seism. Soc. Am.*, **98**, 2469-2481.

Selby ND, & Bowers D. 2013. Assessing the prospective impact of wind turbine generated seismic ground vibration on the detection capability of the EKA seismometer array. Draft paper for submission to journal. In Prep.

Stewart RC. 1988. P-wave seismograms from underground explosions at the Shagan River test site recorded at four arrays. AWE Report O 4/88. 249pp.

Styles P. *et al.* 2005. Microseismic and infrasound monitoring of low frequency noise and vibrations from windfarms. Recommendations of the siting of windfarms in the vicinity of Eskdalemuir, Scotland. Applied and Environmental Geophysics Technical Report, University of Keele. pp125.

Styles P. 2010. An Assessment of the REACTEC/Wind Energy damping system for reduction of ground vibration in the 3 to 6 Hz band and the implications for Eskdalemuir IMS seismometer array station. Applied Environmental Geophysics Technical Report, University of Keele, 47pp.

A Interquartile mean PSD with wind speed — linear plots

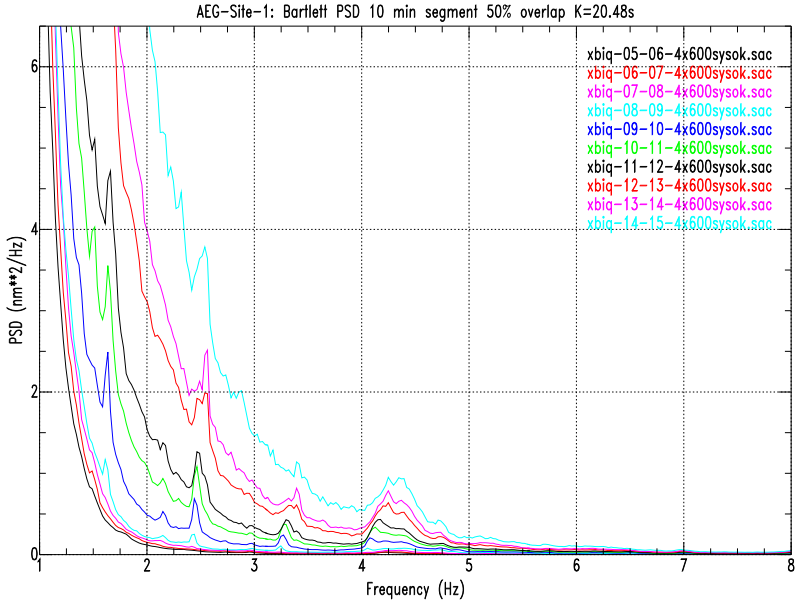

Figure A-1: Comparison of inter-quartile mean vertical displacement PSDs at site AEG-1 with wind speed when all four turbines at Craig are generating electricity.

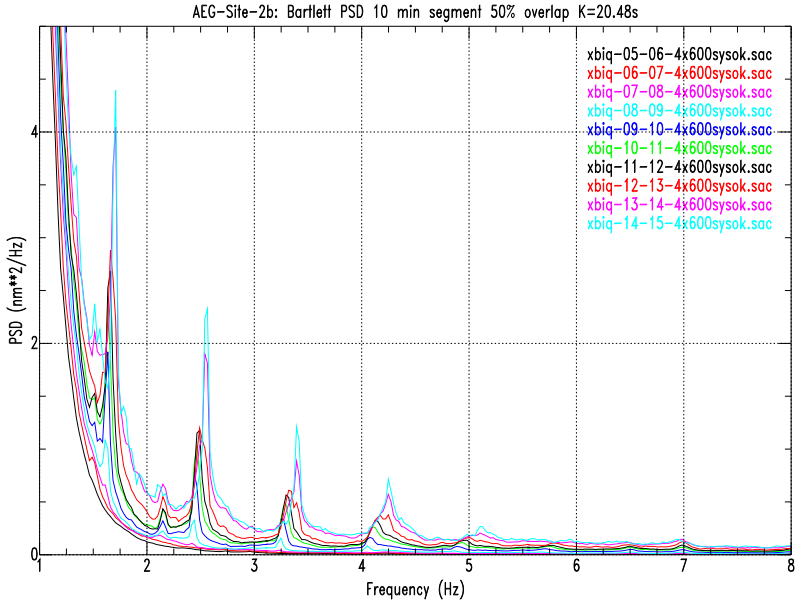

Figure A-2: Comparison of inter-quartile mean vertical displacement PSDs at site AEG-2b with wind speed when all four turbines at Craig are generating electricity.

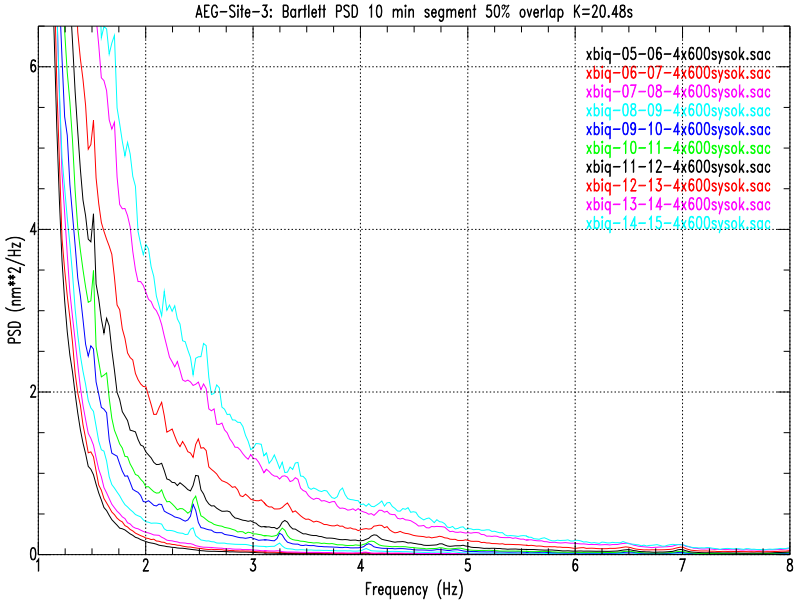

Figure A-3: Comparison of inter-quartile mean vertical displacement PSDs at site AEG-3 with wind speed when all four turbines at Craig are generating electricity.

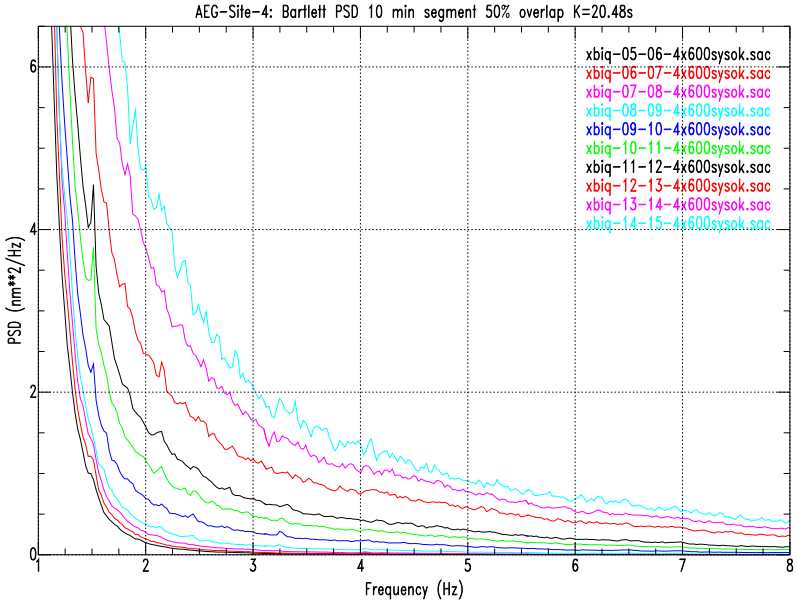

Figure A-4: Comparison of inter-quartile mean vertical displacement PSDs at site AEG-4 with wind speed when all four turbines at Craig are generating electricity.

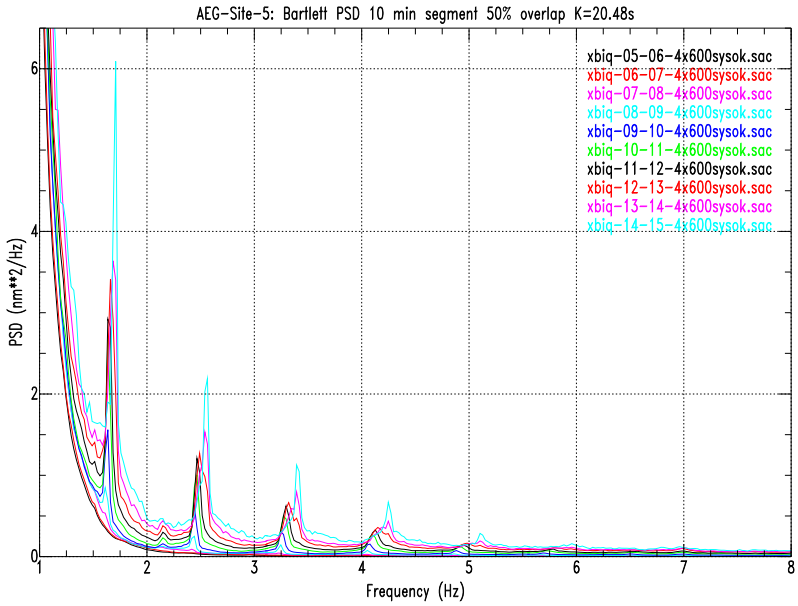

Figure A-5: Comparison of inter-quartile mean vertical displacement PSDs at site AEG-5 with wind speed when all four turbines at Craig are generating electricity.

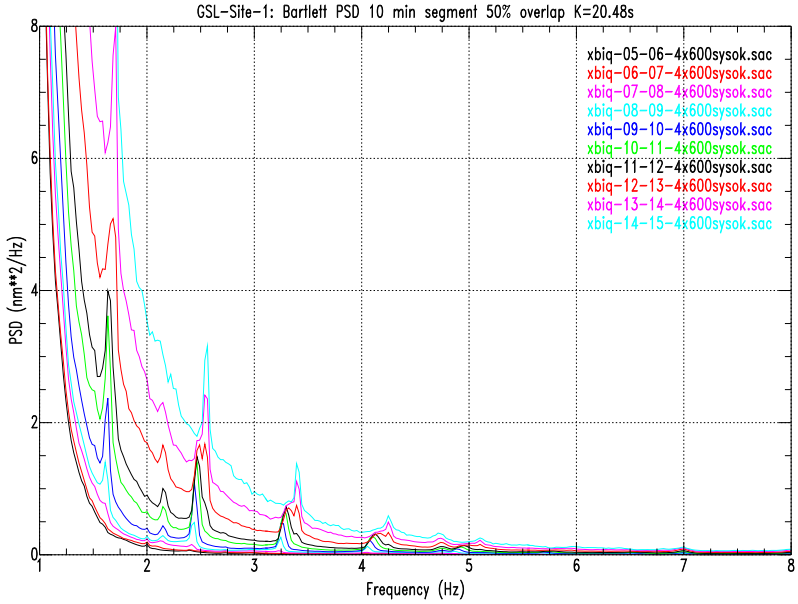

Figure A-6: Comparison of inter-quartile mean vertical displacement PSDs at site GSL-1 with wind speed when all four turbines at Craig are generating electricity.

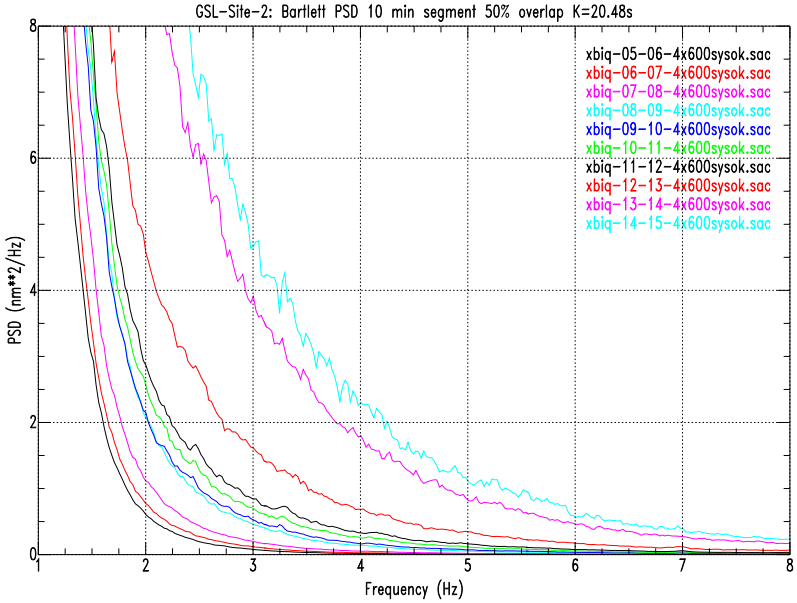

Figure A-7: Comparison of inter-quartile mean vertical displacement PSDs at site GSL-2 with wind speed when all four turbines at Craig are generating electricity.

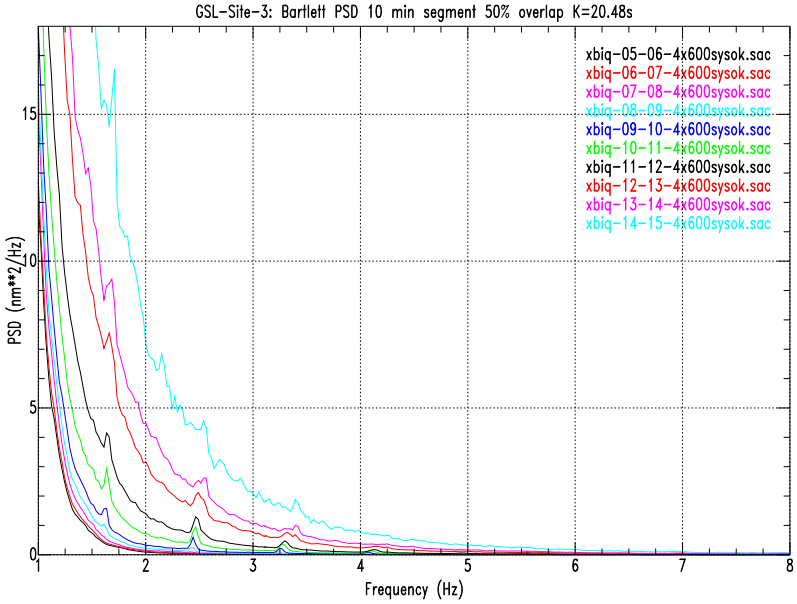

Figure A-8: Comparison of inter-quartile mean vertical displacement PSDs at site GSL-3 with wind speed when all four turbines at Craig are generating electricity.

B Interquartile mean PSD with wind speed — logarithmic plots

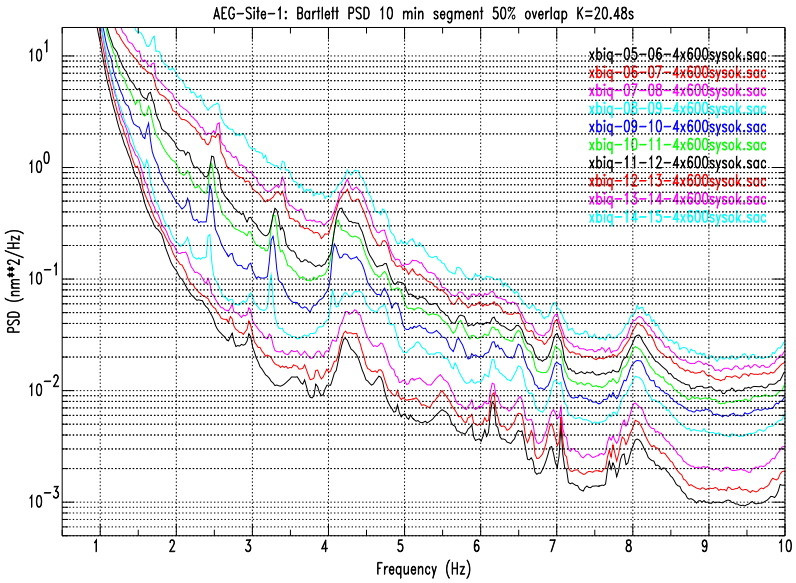

Figure B-1: Comparison of inter-quartile mean vertical displacement PSDs at site AEG-1 with wind speed when all four turbines at Craig are generating electricity.

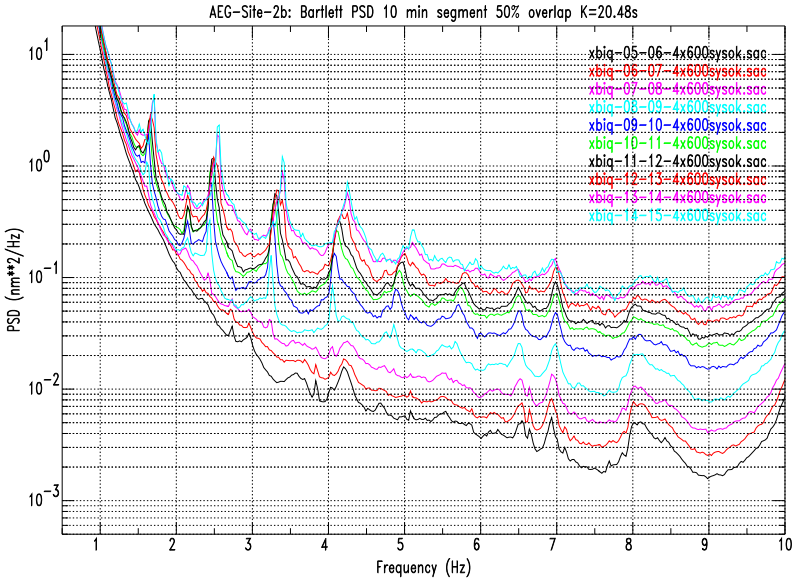

Figure B-2: Comparison of inter-quartile mean vertical displacement PSDs at site AEG-2b with wind speed when all four turbines at Craig are generating electricity.

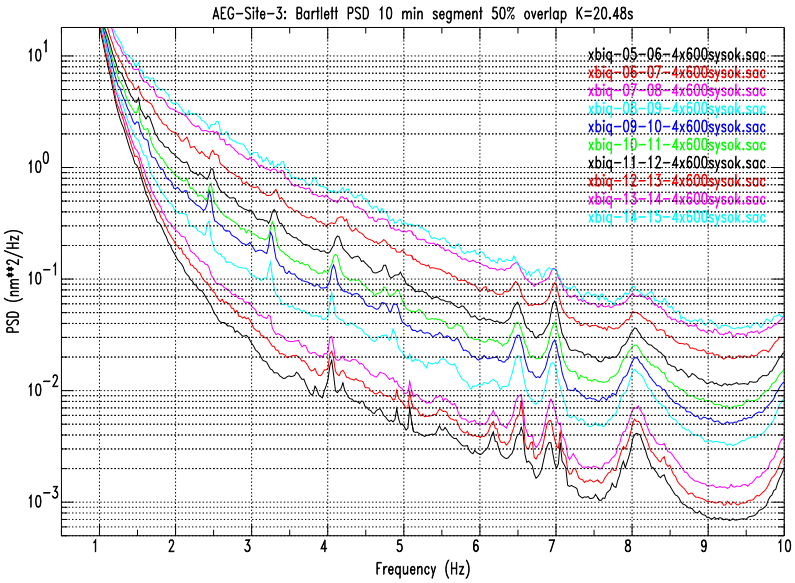

Figure B-3: Comparison of inter-quartile mean vertical displacement PSDs at site AEG-3 with wind speed when all four turbines at Craig are generating electricity.

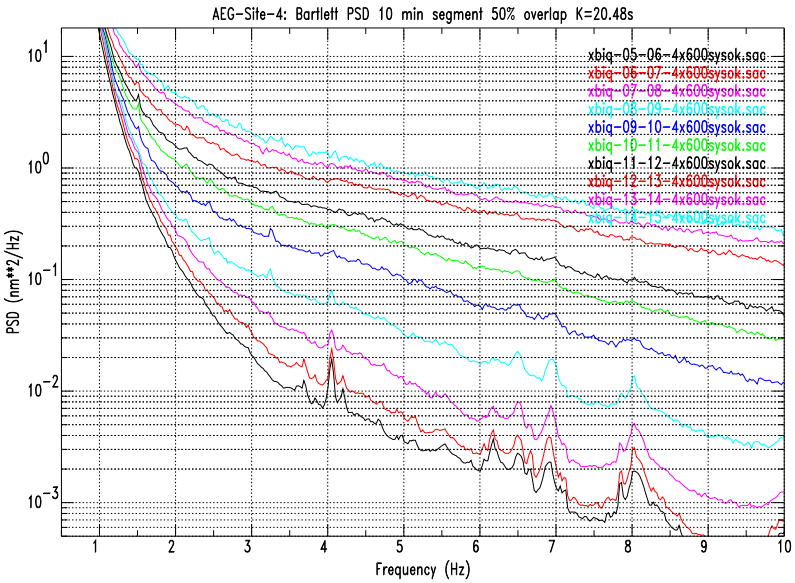

Figure B-4: Comparison of inter-quartile mean vertical displacement PSDs at site AEG-4 with wind speed when all four turbines at Craig are generating electricity.

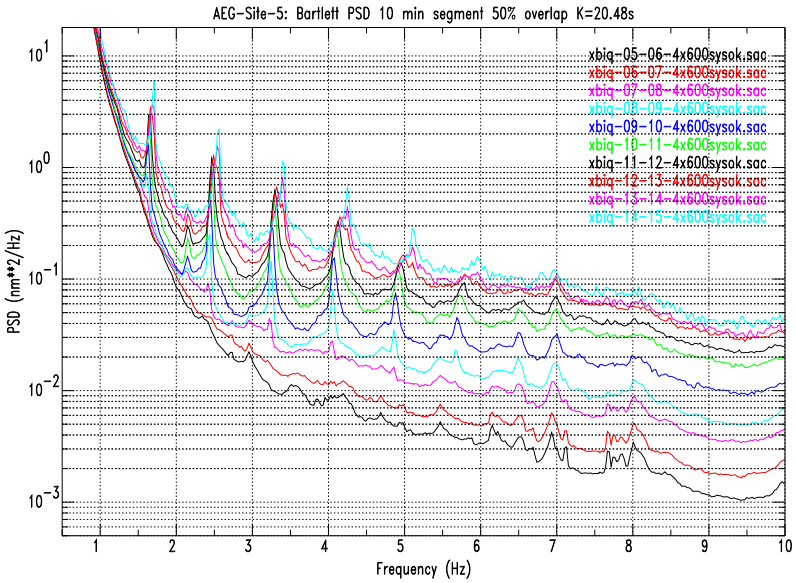

Figure B-5: Comparison of inter-quartile mean vertical displacement PSDs at site AEG-5 with wind speed when all four turbines at Craig are generating electricity.

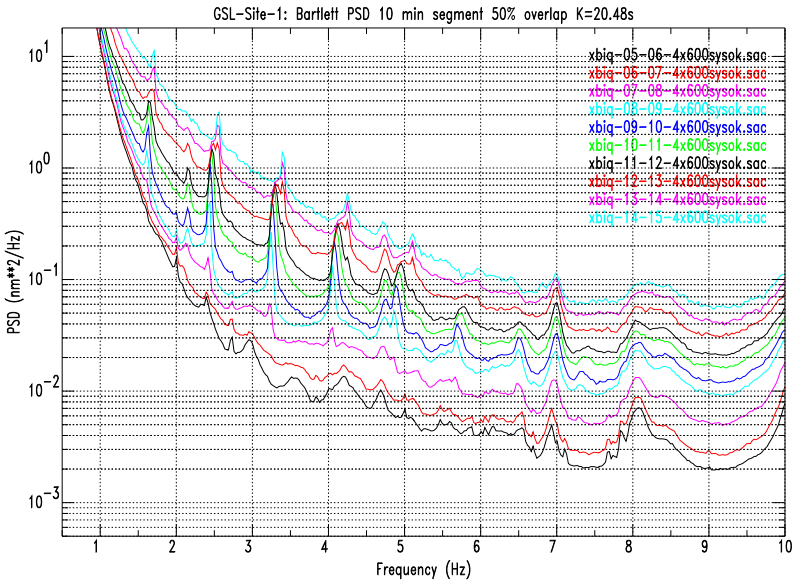

Figure B-6: Comparison of inter-quartile mean vertical displacement PSDs at site GSL-1 with wind speed when all four turbines at Craig are generating electricity.

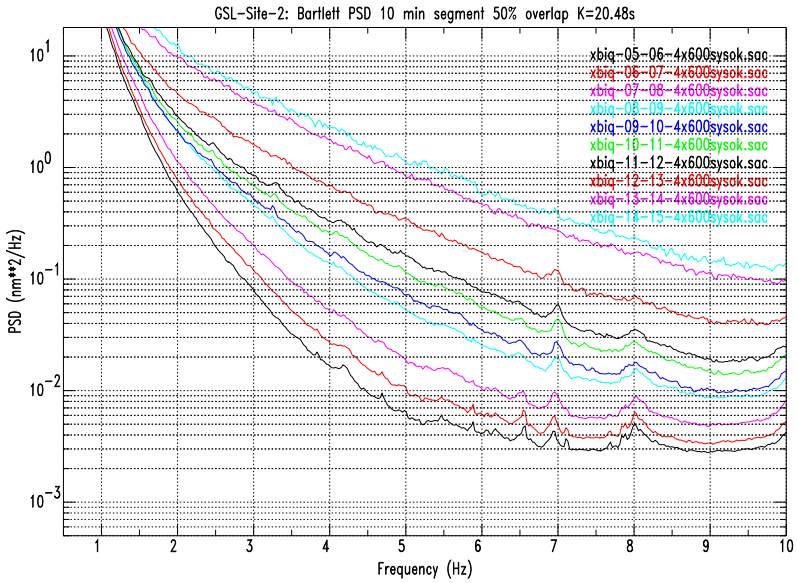

Figure B-7: Comparison of inter-quartile mean vertical displacement PSDs at site GSL-2 with wind speed when all four turbines at Craig are generating electricity.

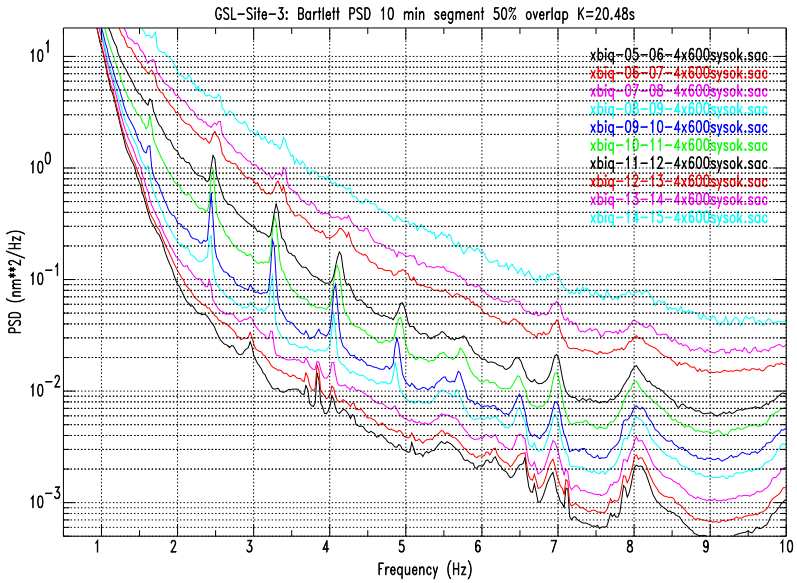

Figure B-8: Comparison of inter-quartile mean vertical displacement PSDs at site GSL-3 with wind speed when all four turbines at Craig are generating electricity.

C Computer programs and scripts

C.1 Frequency-distance weighting Fortran program

Calculates the frequency-distance weights and outputs the final and intermediate stages to ascii (".txt") files and SAC (Seismic Analysis Code) compatible files (".sac")for further analysis. Various other parameters are written to standard output (in a linux environment).

```
      program fdwfsac

c----
c---- Normalisation applied to the freiberger filter
c---- Attenuation term relative to reference distance, including geometrical spreading
c----
c---- OUTPUT SAC FILES fdwf.sac, frei.sac, attpow.sac, noise.sac
c----


      implicit none


c---- FREQUENCY BAND OF INTEREST AND DISCRETIZATION


      real, parameter    :: FNORM = 3.28            ! Normalization frequency.
      real, parameter    :: FMIN  = 0.00            ! Minimum frequency to consider.
      real, parameter    :: FMAX  = 25.0            ! Maximum frequency to consider.
      integer, parameter :: MWIN  = 1024            ! Time window for PSD calculation = 2*MWIN
      integer, parameter :: SAMP  = 50                 ! Sampling rate of time series
      real, parameter    :: DELF  = SAMP / ( 2. * MWIN) ! Frequency step.
      integer, parameter :: NFREQ = MWIN
c

      real :: freq
      real :: fdwf(2048)
      real :: noise(2048)
      real :: frei(2048)
      real :: attpow(2048)
      real :: dummy
```

```
      integer :: nerr


c---- NOISE MODEL

      real    :: noipow               ! Function returning background noise power
                                        at given frequency
      real    :: np                   ! Background seismic noise at particular frequency

c---- Noise model wind speed 11-12m/s, 1348 spectra (Selby & Bowers 2013)

      real, parameter :: A0 =  1.11   ! Coefficients for quadratic describing EKA
                                        background noise power
      real, parameter :: A1 = -8.78   !     "
      real, parameter :: A2 =  3.96   !     "


c---- SIGNAL MODEL

      real, parameter :: CFREQ = 8.0  ! corner frequency of signal of interest.
      real, parameter :: TSTAR = 0.15 ! t*, i.e. apparent attenuation
      real, parameter :: SNR   = 4.0  ! Power SNR

      real :: sigpow                  ! Function returning signal power at given frequency.
      real :: sp                      ! Signal power at particular frequency
      real :: rawsnr, rawsnrmax       ! used to calculate SNR normalization factor
      real :: snrnorm                 ! SNR normalization factor
      real :: peakfreq                ! frequency at peak gain of fdwf
      real :: peakpow                 ! peak filter gain
      real :: peakhalf                ! half peak gain
      real :: fl3db                   ! low-frequency -3dB point
      real :: fh3db                   ! high-frequency -3dB point

      real, parameter :: FCMAX = 6.5  ! Frequency at which beam SNR gain is zero.
      real :: beamcoh                 ! Function which returns beam power/signal power

c---- TURBINE NOISE ATTENUATION

      real, parameter :: Q = 50       ! Attenuation of turbine generated noise
      real, parameter :: U = 2.0      ! Group speed of turbine generated noise
```

```
      real, parameter :: dref=1.0      ! Reference distance (in km) for the turbine
                                         source-term spectrum

      real :: dist                     ! Distance (in km) from turbine to EKA array.
      real :: turbine                  ! Function returning attenuation factor for
                                         turbine generated noise.
      character(len=80) :: cdist

c---- OTHER

      real :: freiberger               ! Function returning value of Freiberger filter;
                                         optimal signal detection filter.
      real :: freinorm                 ! Normalisation factor so that value at freq=FNORM
                                         is unity.

      integer :: ii

      integer :: ipeak



c---- read in the distance in km from turbine to array


      call getarg(1,cdist)
      read(cdist,*) dist


c---- Find signal normalisation so that the maximum (power) SNR is that set above.


      rawsnr = 0.0
      rawsnrmax = 0.0


      do ii = 1, nfreq

         freq = FMIN + real( ii - 1 ) * DELF
         rawsnr =  sigpow(freq,CFREQ,TSTAR,FCMAX)
     1              / noipow(freq,A0,A1,A2)
         rawsnrmax = max(rawsnrmax,rawsnr)
```

```
      enddo


      snrnorm = SNR/rawsnrmax


c---- The freiberger normalisation (freinorm) is the value of the function at
c     frequency=FNORM


      sp = snrnorm * sigpow(FNORM,CFREQ,TSTAR,FCMAX)
      np = noipow(FNORM,A0,A1,A2)

      freinorm = freiberger(sp,np)


      ! Write out the final FDWF, and associated functions, as a function of frequency.


      peakfreq = 0.0
      peakpow = 0.0


      open(16,file='sigpow.txt',status='unknown')
      open(26,file='noipow.txt',status='unknown')
      open(36,file='freiberger.txt',status='unknown')
      open(46,file='beamcoh.txt',status='unknown')
      open(56,file='turbine.txt',status='unknown')
      open(66,file='spovernp.txt',status='unknown')


      do ii = 1 , nfreq

         freq = FMIN + real( ii - 1 ) * DELF

         np = noipow(freq,A0,A1,A2)
         sp = sigpow(freq,CFREQ,TSTAR,FCMAX) * snrnorm

c clean up np +infty out of range
         if(freq.le.0.5) np=99999.
```

```
         noise(ii) = np

         frei(ii) = freiberger(sp,np) / freinorm

         attpow(ii) = turbine(freq,Q,U,dist,dref)

         fdwf(ii) = frei(ii) * attpow(ii)

         if (fdwf(ii).gt.peakpow) then
            peakfreq = freq
            peakpow = fdwf(ii)
            ipeak=ii
         endif

         write(16,*) freq, sp
         write(26,*) freq, np
         write(36,*) freq, freiberger(sp,np)
         write(46,*) freq, beamcoh(freq,FCMAX)
         write(56,*) freq, turbine(freq,Q,U,dist,dref)
         write(66,*) freq, sp/np

c         write(*,*) ii, freq, fdwf(ii)

      enddo

      write(*,*) peakpow,peakfreq

c        3dB "corner" frequencies

      peakhalf = peakpow * 0.5

      do ii = ipeak, 1, -1

         freq = FMIN + real( ii - 1 ) * DELF

         if (fdwf(ii).ge.peakhalf) then
            fl3db = freq
         endif
      enddo
```

```
      do ii = ipeak, nfreq

         freq = FMIN + real( ii - 1 ) * DELF

         if (fdwf(ii).ge.peakhalf) then
            fh3db = freq
         endif
      enddo

      write(*,*) fl3db, fh3db, fh3db-fl3db


      close(16)
      close(26)
      close(36)
      close(46)
      close(56)
      close(66)

c---- Set up SAC headers etc.

          call newhdr()
          call setlhv('leven',.true.,nerr)
          call setfhv('b',FMIN,nerr)
          call setfhv('delta',DELF,nerr)
          call setnhv('npts',MWIN,nerr)
          call setihv('iftype','ixy',nerr)
          call wsac0('noise.sac',dummy,noise,nerr)
          call wsac0('attpow.sac',dummy,attpow,nerr)
          call wsac0('frei.sac',dummy,frei,nerr)
          call setfhv('user0',dist,nerr)
          call setfhv('user1',peakfreq,nerr)
          call wsac0('fdwf.sac',dummy,fdwf,nerr)

      end


c-----------------------------------------------------------------------


      function freiberger(sp,np)
```

```
c---- Freiberger (power) filter: optimal signal detection filter for given
c---- signal and noise power.

      implicit none

      real :: freiberger, sp, np

      freiberger = ( sp/np ) / ( sp + np )

      return
      end

c----------------------------------------------------------------------

      function turbine(f,Q,U,dist,dref)

c---- Returns the relative attenuation factor from dref as a function of distance.
c---- Includes geometrical spreading (assuming cylindrical spreading)

      implicit none

      real, parameter :: PI = 3.141592654
      real :: turbine, f, dist, Q, U, dref

      turbine = (dref / dist) * ( exp( ( -1.0 * PI * f * (dist - dref) ) / ( Q * U ) ) )**2

      return
      end
```

```
c-----------------------------------------------------------------------

      function sigpow(f,CFREQ,TSTAR,FCMAX)

c---- Teleseismic signal power spectrum on the beam at EKA

      implicit none

      real :: sigpow
      real :: f, CFREQ, TSTAR, FCMAX
      real :: beamcoh

      real, parameter :: PI =  3.141592654
      real, parameter :: EL =  0.0          ! signal power exponent below corner frequency
      real, parameter :: EH = -2.0          ! signal power exponent above corner frequency

      real :: refh, refl



      refh =  CFREQ ** EH
      refl =  CFREQ ** EL


      if( f .lt. CFREQ ) then

         sigpow = ( ( f ** EL / refl ) * exp( -1.0 * PI * f * TSTAR ) ) ** 2

      else if( f .ge. CFREQ ) then

         sigpow = ( ( f ** EH / refh ) * exp( -1.0 * PI * f * TSTAR ) ) ** 2

      endif


      sigpow = sigpow * beamcoh(f,FCMAX)
```

```
      return
      end


c---------------------------------------------------------------------

      function noipow(f,A0,A1,A2)

c---  Background seismic noise power spectrum at EKA

      implicit none

      real :: noipow, f
      real :: A0, A1, A2
      real :: x



      x      = log10(f)
      noipow = 10**( A0 + A1*x + A2*x*x )

      return
      end

c---------------------------------------------------------------------

      function beamcoh(f,FCMAX)

c---- Returns the ratio of beam power to (single channel) signal power.
```

```
      implicit none


      real :: beamcoh, f, FCMAX

      real, parameter    :: PI    = 3.141592654
      integer, parameter :: NCHAN = 20                ! Number of channels at EKA; fixed.



      if( f .lt. FCMAX ) then

         beamcoh = (1.0/real(nchan)) +
     1      (real(nchan-1)/real(2*nchan))*( 1.0 + cos(PI*f/FCMAX) )

      else

         beamcoh = ( 1.0/real(nchan) )

      endif


      return
      end
```